SANDIA NATIONAL LABORATORIES

WASTE ISOLATION PILOT PLANT

ANALYSIS PACKAGE FOR NORMALIZED RELEASES IN THE 2019 COMPLIANCE RECERTIFICATION APPLICATION PERFORMANCE ASSESSMENT (CRA-2019 PA)

REVISION 0

	Print	Signature	Date
Author:	Sarah Brunell	Sarah Brunell	8/26/2019
Technical Reviewer:	Todd R. Zeitler	Sarah Brunell for	8/26/2019
QA Reviewer:	Shelly Nielsen	Shelly R. Nielsen	8-26-19
Management Reviewer:	Chris Camphouse	Brad Day for	8/26/19

ERMS #571373

AUGUST 26, 2019

WIPP:4.2.1:PA:QA-L:571155

This page intentionally left blank.

TABLE OF CONTENTS

LIST OF TABLES

LIST OF FIGURES

This page intentionally left blank.

Executive Summary

The Land Withdrawal Act requires that the U.S. Department of Energy (DOE) apply for recertification of the Waste Isolation Pilot Plant (WIPP) every five years following the initial 1999 waste shipment. The 2019 Compliance Recertification Application (CRA-2019) is the fourth WIPP recertification application submitted for approval by the U.S. Environmental Protection Agency. A performance assessment (PA) has been executed by Sandia National Laboratories in support of the DOE submittal of the CRA-2019. Results found in the CRA-2019 PA are compared to those obtained in the 2014 Compliance Recertification Application (CRA-2014) in order to assess repository performance in terms of the current regulatory baseline. This package documents the CCDF creation component of the CRA-2019 PA. Changes incorporated into the CRA-2019 PA include repository planned changes, parameter updates, and refinements to PA implementation. Many of these changes affect normalized releases. The changes included in the CRA-2019 PA that directly affect the CCDFGF creation component of CRA-2019 PA compared to the CRA-2014 PA are:

- Inclusion of an approach to accommodate the operational decisions to not emplace panel closures in Panels 3, 4, 5, and 6 and to not emplace waste in Panel 9.
- Refinement to the probability of encountering pressurized brine.
- Updates to drilling rate and plugging pattern parameters.
- Hardware and computational code updates.

CCDFGF was used to generate complementary cumulative distribution functions (CCDFs) for three replicates, each containing 100 vectors for the CRA19 analysis of the CRA-2019 PA. The CCDF provides the probability of the variable being greater than a particular value. By regulation, performance assessment results are presented as a distribution of CCDFs of releases (U.S. EPA 1996). The overall mean CCDF is computed as the arithmetic mean of the three mean CCDFs from each replicate. Confidence limits are computed about the overall mean CCDF using the Student's t-distribution, the mean CCDFs from each replicate, and the standard error based on the three replicate means. As described in 40 CFR Part 194, the key metric for regulatory compliance is this overall mean CCDF for total releases in combination with its confidence limits.

Total mean releases, as well as mean releases by each individual release mechanism, have increased for the CRA-2019 PA at all probabilities. The largest increases are seen from spallings release and direct brine release (DBR) contributions, the latter being a dominant contributing factor to overall releases. Although cuttings and cavings is another dominant release mechanism, both cuttings and cavings and transport releases showed only a slight increase. Overall, the primary impacts on the CRA-2019 PA in comparison to the CRA-2014 PA baseline are due to increased waste area brine pressures and saturations (from a number of sources), as well as the increased drilling rate and probability of a borehole intersecting brine. The main impacts to brine pressures and saturations came from the lack of panel closures in the south end of the repository, the introduction of radiolysis as a source of gas generation, and updated iron corrosion rates. Releases were decreased to some degree by the changes in plugging pattern parameters. Total normalized releases calculated in the CRA-2019 PA remain below their regulatory limits. As a result, the WIPP remains in compliance with the containment requirements of 40 CFR Part 191.

This page intentionally left blank.

1.0 INTRODUCTION

The Waste Isolation Pilot Plant (WIPP), located in southeastern New Mexico, has been developed by the U.S. Department of Energy (DOE) for the geologic (deep underground) disposal of transuranic (TRU) waste. Containment of TRU waste at the WIPP is regulated by the U.S. Environmental Protection Agency (EPA) according to the regulations set forth in Title 40 of the Code of Federal Regulations (CFR), Part 191. The DOE demonstrates compliance with the containment requirements according to the Certification Criteria in Title 40 CFR Part 194 by means of performance assessment (PA) calculations performed by Sandia National Laboratories (SNL). WIPP PA calculations estimate the probability and consequence of potential radionuclide releases from the repository to the accessible environment for a regulatory period of 10,000 years after facility closure. The models used in PA are maintained and updated with new information as part of an ongoing process. Improved information regarding important WIPP features, events, and processes typically results in refinements and modifications to PA models and the parameters used in them. Planned changes to the repository and/or the components therein also result in updates to WIPP PA models. WIPP PA models are used to support the repository recertification process that occurs at five-year intervals following the receipt of the first waste shipment at the site in 1999.

PA calculations were included in the 1996 Compliance Certification Application (CCA) (U.S. DOE 1996), and in a subsequent Performance Assessment Verification Test (PAVT) (MacKinnon and Freeze 1997a, 1997b, and 1997c). Based in part on the CCA and PAVT PA calculations, the EPA certified that the WIPP met the regulatory containment criteria. The facility was approved for disposal of transuranic waste in May 1998 (U.S. EPA, 1998). PA calculations were an integral part of the 2004 Compliance Recertification Application (CRA-2004) (U.S. DOE 2004). During their review of the CRA-2004, the EPA requested an additional PA calculation, referred to as the CRA-2004 Performance Assessment Baseline Calculation (PABC) (Leigh et al. 2005), be conducted with modified assumptions and parameter values (Cotsworth 2005). Following review of the CRA-2004 and the CRA-2004 PABC, the EPA recertified the WIPP in March 2006 (U.S. EPA 2006).

PA calculations were completed for the second WIPP recertification and documented in the 2009 Compliance Recertification Application (CRA-2009). The CRA-2009 PA resulted from continued review of the CRA-2004 PABC, including a number of technical changes and corrections, as well as updates to parameters and improvements to the PA computer codes (Clayton et al., 2008). To incorporate additional information which was received after the CRA-2009 PA was completed, but before the submittal of the CRA-2009, the EPA requested an additional PA calculation, referred to as the 2009 Compliance Recertification Application Performance Assessment Baseline Calculation (PABC-2009) (Clayton et al. 2010), be undertaken which included updated information (Cotsworth 2009). Following the completion and submission of the PABC-2009, the WIPP was recertified in 2010 (U.S. EPA 2010).

PA calculations were completed for the third WIPP recertification and documented in the 2014 Compliance Recertification Application (CRA-2014). Following the completion and submission of the CRA-2014, the WIPP was recertified in 2017 (U.S. EPA 2017a).

The Land Withdrawal Act (U.S. Congress 1992) requires that the DOE apply for WIPP recertification every five years following the initial 1999 waste shipment. The 2019 Compliance Recertification Application (CRA-2019) is the fourth WIPP recertification application submitted by the DOE for EPA approval. The PA executed by SNL in support of the CRA-2019 is detailed in AP-181 (Zeitler 2019c). The CRA-2019 PA includes repository planned changes, parameter updates, and refinements to PA implementation. Results found in the CRA-2019 PA are compared to those obtained in the CRA-2014 in order to assess repository performance in terms of the current regulatory baseline. This analysis package documents the CCDF creation component of the CRA-2019 PA analysis.

1.1 Changes Since the CRA-2014

Several changes were incorporated in the CRA-2019 PA relative to the CRA-2014 PA that potentially have an impact on releases from the repository. These modifications include repository planned changes, parameter updates, and refinements to PA implementation. More specifically, changes included in the CRA-2019 PA include the following:

- Inclusion of an approach to accommodate the operational decisions to not emplace panel closures in Panels 3, 4, 5, and 6 and to not emplace waste in Panel 9.
- Inclusion of an approach to accommodate an additional shaft connecting the repository to the surface, as well as an additional mined region in the repository north end to accommodate drifts that lead to the new shaft.
- Refinement of the gas generation process model to include brine radiolysis.
- An update to the probability that a drilling intrusion into a repository excavated region will intersect the Castile brine reservoir modeled in BRAGFLO
- Refinement to the corrosion rates of steel under humid and inundated conditions
- Refinement to the effective shear strength of WIPP waste
- Refinement to colloid enhancement parameters associated with actinide mobilization
- Refinement to the hydromagnesite to magnesite conversion rate
- Removal of two chemical reactions associated with iron sulfidation
- Correction to the length of the northernmost panel closure representation in the BRAGFLO grid
- Updates to drilling rate and plugging pattern parameters.
- Updates to WIPP waste inventory parameters.
- Updates to radionuclide solubilities and their associated uncertainty.
- An update to the BH_OPEN:RELP_MOD parameter
- Introduction of new materials to define properties in some disturbed rock zone areas
- Hardware and computational code updates.

All of these changes (with the exception of defining new materials in DRZ areas) potentially have an impact on releases from the repository, primarily via impact to results from codes run prior to CCDFGF. Several changes are incorporated in the CRA-2019 PA relative to the CRA-2014 PA that are directly used by the CCDFGF code. The changes are:

- Inclusion of an approach to accommodate the operational decisions to not emplace panel closures in Panels 3, 4, 5, and 6 and to not emplace waste in Panel 9.
- Refinement to the probability of encountering pressurized brine.
- Updates to drilling rate and plugging pattern parameters.
- Hardware and computational code updates.

The changes listed above are discussed in more detail in the sections that follow.

1.1.1 The Abandonment of Panel Closures in the South and No Waste in Panel 9

As outlined in the CRA-2019 analysis plan (Zeitler 2019c), the WIPP repository was closed in February 2014 and later reopened on a limited basis, which resulted in maintenance delays in the repository. The DOE has proposed an operational policy change at WIPP as a result of the severe ground control issues caused by the maintenance delays. The policy change prohibits personnel access to (with the ultimate goal of withdrawal from) the area in the WIPP underground designated as equivalent Panel 9 (U.S. DOE 2016). With that change, the planned implementation of run-of-mine salt panel closures (ROMPCS) in Panels 3, 4, 5, and 6 would no longer be possible. Also, waste emplacement in the area designated as Panel 9 would no longer be possible. In response to the operational changes, the DOE requested that SNL undertake calculations and analyses to determine the impacts of the proposed changes to the repository configuration on the long-term performance of the facility (U.S. DOE 2017). The approach to modeling the impacts of the operational changes and the results of the Abandonment of Panel Closures in South End of Repository (APCS) analysis are described in Zeitler et al. (2017). The piece of the APCS approach that directly impacts CCDFGF calculations is that of "panel reneighboring."

The APCS approach considered the removal of waste from Panel 9 and relocation of waste to a new panel somewhere north of Panel 8, outside of the current repository configuration. It was shown to be appropriately conservative with respect to releases to continue to model waste within the existing Panel 9 in lieu of adding new waste panel(s) to the north. The conservatism was attributed to the 1-degree (south) dip in the Salado formation, which results in increased brine accumulation due to gravity drainage, increased hydrostatic pressure, and increased gas generation due to corrosion (enabled by the increased availability of brine) at the deeper/south portion of the repository. Previous PA analyses consistently show increasing brine saturations and pressures in the repository when moving from the north to the south. Thus, continuing to model the same mass of waste as if it is located in Panel 9 results in somewhat larger DBR and spallings releases compared to if the same mass was relocated to an arbitrary location further north. In the APCS analysis, this conservatism was greatly enhanced due to the abandonment of panel closures between Panels 3, 4, 5, 6, and 9, which effectively equilibrates the brine pressures and saturations in those panels. The APCS analysis also showed that the potential nonconservative condition of not considering DBRs from both the empty Panel 9 and the hypothetical Panel 9 replacement is more than covered by the conservative assumptions of the panel neighbor redefinitions. For CRA-2019 PA calculations, it is considered to be appropriately conservative with respect to releases to continue to model waste within the existing Panel 9 in lieu of adding new waste panel(s) to the north.

1.1.2 Additional Shaft and Associated Drifts

In the wake of the 2014 radiological release event at the WIPP site, a modified ventilation system is planned that will provide sufficient airflow necessary for the resumption of increased-rate disposal operations in the future. The primary components of the modified ventilation system are an additional shaft in the north end of the repository and associated drifts to connect the additional shaft to the experimental area of the repository.

There are four shafts currently located in the repository north end, namely a salt handling shaft, an exhaust shaft, a waste shaft, and an air intake shaft. In WIPP PA, these shafts are combined into a single shaft that captures the combined impacts of all of them. The additional, planned shaft will be combined with the four existing shafts in the CRA-2019 PA. Additionally, mined volume in the repository north end will be modified in the repository representation so as to include the additional drifts created to access the new shaft. A similar approach was employed for the SHFT14 analysis that accompanied a planned change notice (PCN) submitted to the EPA in 2017 (Camphouse 2014). That analysis showed minimum impact to the long-term repository performance from representing the additional shaft and drifts. Updated model dimensions for the shaft and experimental area representations to be used in the BRAGFLO Salado grid were derived by Zeitler (2019a), and its impacts to the CRA19 analysis are described in Day (2019b).

1.1.3 Brine Radiolysis as Part of Gas Generation Process Model

A recent scoping analysis has identified a need to include radiolytic gas generation in WIPP PA (Day 2019a). Therefore brine radiolysis was included in the CRA-2019 PA as part of the gas generation process model. The implementation and associated assumptions are described in detail in Day (2019a). Its impacts to Salado flow are described in Day (2019b) and to spallings volumes are described in Kicker (2019a).

1.1.4 Refinement to the Probability of Encountering Pressurized Brine

The WIPP PA parameter GLOBAL:PBRINE (hereafter PBRINE) is used to specify the probability that a drilling intrusion into the excavated region of the repository encounters a region of pressurized brine below the repository. Development of the distribution for PBRINE used prior to the CRA-2014 PA was the result of an analysis of TDEM data (Rechard et al. 1991, Peake 1998). A framework that provided a quantitative argument for refinement of the PBRINE parameter was developed for the CRA-2014 PA (Kirchner et al. 2012). The refinement of PBRINE resulted from a re-examination of the TDEM data while also including a greatly expanded set of drilling data for locations adjacent to the WIPP site than were available when the original analysis was performed in 1998. The EPA has since created a revised distribution for the PBRINE parameter based on a reexamination of the original TDEM data and recommended its use in the CRA-2019 PA. The resulting cumulative distribution for PBRINE is described in detail in U.S. EPA (2017b) and summarized in Zeitler (2019b) (Table 1). The DOE has agreed to use of the U.S. EPA-identified distribution in the CRA-2019 PA. The EPA previously directed this distribution for use by the DOE as part of the CRA14_SEN4 sensitivity study, and it was found that the range of values sampled from the CRA14_SEN4 distribution encompasses that from CRA14, but predominantly consists of values higher than those used in CRA14 (Zeitler and Day 2016).

Table 1 – GLOBAL:PBRINE Distribution

Material	Property	Description	Units	CRA-2014 Value	CRA-2019 Value
GLOBAL	PBRINE	Probability that Drilling Intrusion in Excavated Area Encounters Pressurized Brine	None	Normal Distribution	Cumulative Distribution

1.1.5 Refinement to the Corrosion Rates of Steel

The interaction of steel in the WIPP with repository brines will result in the formation of H_2 gas due to anoxic corrosion of the metal. Two steel corrosion rates were updated for the CRA-2019 PA, STEEL:CORRMCO2 and STEEL:HUMCORR. The effect of these changes on the CRA19 analysis are described in Day (2019b) and Kicker (2019a).

1.1.6 Refinement to the Effective Shear Strength of WIPP Waste

WIPP PA includes scenarios in which human intrusion results in a borehole intersecting the repository. During the intrusion, drilling mud flowing up the borehole will apply a hydrodynamic shear stress on the borehole wall. Erosion of the wall material can occur if this stress is high enough, resulting in a release of radionuclides being carried up the borehole with the drilling mud. The WIPP PA parameter BOREHOLE:TAUFAIL (hereafter TAUFAIL) is used to represent the effective shear strength for erosion of WIPP waste. Kicker (2019a) and Zeitler (2019b) include discussions on the effect of this change on the CRA19 analysis.

1.1.7 Refinement to Colloid Enhancement Parameters

Refinements to the colloid enhancement parameters impact mobilized radionuclide concentrations used for DBRs and are detailed in Sarathi (2019). They also impact the Salado flow solution through the inclusion of brine radiolysis which is in part dependent upon the quantity of each contributing radionuclide in the waste area brine.

1.1.8 Refinement to Hydromagnesite Conversion Rate

For the CRA-2014 PA, the reaction of hydromagnesite to form magnesite was included along with an associated reaction rate, parameterized as WAS_AREA:HYMAGCON (hereafter

HYMAGCON), derived by Clayton (2013). Subsequent to the submittal of the CRA-2014, the EPA requested that the DOE revise the distribution for HYMAGCON. A revised distribution was provided to the EPA by the DOE, but the EPA recommended a different distribution for the CRA-2019 PA (U.S. EPA 2017c). The uniform distribution used for HYMAGCON in the CRA-2019 PA is described in U.S. EPA (2017c) and summarized in Zeitler (2019b), and a description of the effects of this change is described in Day (2019b). The conversion rate impacts water balance and thus Salado flow solutions.

1.1.9 Removal of Iron Sulfidation Reactions

For the CRA-2014 PA, the sulfidation reactions with iron and iron hydroxide were included as part of the repository brine and gas production/consumption calculations. Subsequent to the submittal of the CRA-2014, the EPA requested that the DOE remove these chemical reactions from WIPP PA by setting the appropriate stoichiometric coefficients (i.e., REFCON:STCO_31, REFCON:STCO_32, REFCON: STCO_35, REFCON:STCO_36, REFCON:STCO_43, and REFCON:STCO_46) to zero. The request to remove iron sulfidation reactions from WIPP PA and the impact to WIPP PA parameters for the CRA-2019 PA is described in U.S. EPA (2017b) and summarized in Zeitler (2019b), the effects of this change on the CRA19 analysis are discussed in Day (2019b). The removal of iron sulfidation reactions impacts water balance and thus Salado flow solutions.

1.1.10 Correction to the Length of Northernmost Panel Closure Representation

Three separate panel closure areas are modeled in BRAGFLO. The "northernmost" panel closure area separates the operations area from the "north rest of repository" (NROR) waste area, the "middle" panel closure separates the NROR from the "south rest of repository" (SROR), and the "southernmost" panel closure separates the SROR from the waste panel.

As part of the DOE/EPA completeness determination discussions for CRA-2014, an error in the length of the northernmost panel closure was identified by the DOE—the northernmost panel closure in the BRAGFLO grid should represent the length of two panel closures. This is done to represent the combined blockage corresponding to the set of panel closures directly north of Panel 10 and the set of closures between the operations and experimental areas. A discussion of the implementation of this change is found in Day (2019b) and is summarized in Zeitler (2019a).

1.1.11 Updates to Drilling Rate and Plugging Pattern Parameters

WIPP regulations require that current drilling practices be assumed for future inadvertent intrusions. The DOE continues to survey drilling activity in the Delaware Basin in accordance with the criteria established in 40 CFR 194.33. Local well operators are surveyed annually to provide the WIPP project with information on drilling practices, Castile brine encounters, etc. Survey results through September 2018 are documented in the 2018 Delaware Basin Monitoring Annual Report (DBMAR) (DOE 2018).

Drilling parameters were updated for the CRA-2019 PA to include information assembled through September 2018. The 2018 DBMAR indicates a drilling rate of 99.0 boreholes per km^2

over 10,000 years, resulting in a value for WIPP PA parameter GLOBAL:LAMBDAD of 9.90×10^{-3} boreholes per km^2 per year for the CRA-2019 PA, a notable increase to the value of 6.73×10^{-3} specified for this parameter in the CRA-2014 PA.

Borehole plugging pattern parameters were also updated based on data contained in the 2018 DBMAR. The DBMAR reports six types of plugging patterns (summarized in Table 9 of the DBMAR), which have historically been translated into three unique plugging patterns for PA purposes. This same translation scheme (i.e., type VI is the same as a full plug, types II and IV are the same as a two-plug, and types I, III, and V are the same as a three-plug configuration) were used for the parameterization of the GLOBAL:ONEPLG, GLOBAL:TWOPLG, and GLOBAL:THREEPLG parameters for the CRA-2019 PA. Selection by the CCDFGF code of ONEPLG leads to an E0 scenario, while selection of THREEPLG leads to an E2 scenario. Selection of TWOPLG leads to either an E1 or E2 scenario depending on the sampled value of the PBRINE parameter (Section 1.1.4). See SNL (2010) for a description of the use of the plugging pattern parameters in WIPP PA.

Although the translation scheme remains the same as for the CRA-2014 PA, the DOE has made a change to the physical area over which plugging pattern data are collected. The DBMAR states that the new dataset "more accurately represents plugging techniques and activities used in the vicinity of the WIPP and is consistent with the provisions of 40 CFR 194.33(c)(1) and the future states assumptions of 40 CFR 194.25" (DOE 2018). As a result, the plugging pattern dataset is somewhat different than in previous versions of the DBMAR. Because of the substantial and potentially impactful changes of the drilling parameters, comparison values from the CRA-2014 PA are also presented in Table 2.

Table 2 – Drilling Rate and Plugging Pattern Parameters

Material	Property	Description	Units	CRA-2014 Value	CRA-2019 Value
GLOBAL	LAMBDAD	Drilling rate per unit area	km^{-2} yr^{-1}	6.73×10^{-3}	9.90×10^{-3}
GLOBAL	ONEPLG	Probability of having Plug Pattern 1 (full plug)	None	0.04	0.403
GLOBAL	TWOPLG	Probability of having Plug Pattern 2	None	0.594	0.331
GLOBAL	THREEPLG	Probability of having Plug Pattern 3	None	0.366	0.266

1.1.12 Updates to WIPP Waste Inventory Parameters

The Performance Assessment Inventory Report (PAIR) - 2018 (Van Soest 2018) was released on December 20, 2018. The PAIR-2018 contains updated estimates to the radionuclide content and waste material parameters, scaled to a full repository, based on inventory information collected up to December 31, 2017. In order to incorporate this update to the inventory into the CRA-2019 PA, the parameters for the initial radionuclide, chemical component and waste material inventories will be updated. In addition, parameters which are calculated based on the initial radionuclide inventories, such as the Waste Unit Factor (WUF) and the initial lumped radionuclide inventories, will be updated as well. This update to the WUF is described in Table 3 and in Kicker (2019c). Impacts resulting from changes to the other parameters can be found in Day (2019b), Kicker (2019a), and Sarathi (2019).

Table 3 – BOREHOLE:WUF Parameter Value for the CRA-2019 PA

Material	Property	Description	Units	CRA-2014 Value	CRA-2019 Value
BOREHOLE	WUF	Waste Unit Factor	None	2.06	3.30

1.1.13 Updates to Radionuclide Solubilities

Updates to radionuclide solubilities (baseline values and associated uncertainties) impact mobilized radionuclide concentrations used for DBRs and are detailed in Sarathi (2019). They also impact the Salado flow solution through the inclusion of brine radiolysis which is in part dependent upon the quantity of each contributing radionuclide in the waste area brine (Day 2019b).

1.1.14 An Update to the BH_OPEN:RELP_MOD Parameter

A minor error in the BRAGFLO code related to the calculation of capillary pressure was discovered, as detailed in software problem report (SPR) 18-002, and determined to have an insignificant effect on repository performance results (Day 2018).

1.1.15 Introduction of New Materials to Define Properties in Some Disturbed Rock Zone Areas

As part of their review of the CRA-2014, the EPA directed multiple sensitivity studies that investigated impacts of parameter changes to the OPS, EXP, and panel closure areas and their associated disturbed-rock zones (DRZs), while leaving the DRZ surrounding the waste panel unchanged. To facilitate those analyses, new material names were used that introduced flexibility in specifying material properties independently across areas for which material properties in the CRA-2014 PA were identical. The flexibility of managing material properties by using these new material names will be preserved in the CRA-2019 PA. Because these changes were only made to naming materials, not the properties associated with them, there is no effect on the CRA19 analysis.

1.1.16 Hardware and Computational Code Updates

CRA-2014 PA calculations were done on the WIPP PA computing cluster running a VMS operating system **(**Long 2013**)**. WIPP PA codes have since been migrated to a cluster running a Solaris operating system (Kirchner 2012, Kirchner et al. 2014, Kirchner et al. 2015). As part of the migration effort, CRA-2014 PA calculations were rerun on the Solaris system with results saved in the official results database (PA_Results) as Revision 0 (Kirchner et al. 2014). After correcting an error that existed in the version of the DRSPALL code used in the original CRA-2014 PA calculations, CRA-2014 PA calculations were again rerun on Solaris and the results were saved as Revision 1 (spallings releases had increased, but total releases were not substantially changed) (Kirchner et al. 2015). Also, as part of the migration effort, an updated version of the CCDFGF code (version 7.02) was migrated to the Solaris system and the CRA-2014 PA (Rev. 1) results were used as input to updated CRA-2014 calculations, the results of which were saved as Revision 2 (no releases were substantially different from the Rev. 1 results) (Kirchner et al. 2015). The baseline for comparison of CRA-2019 PA results is the CRA-2014 PA results as calculated on the new WIPP PA Solaris system with the correction to the DRSPALL results and updated version of CCDFGF (i.e., CRA-2014, Rev. 2).

Additional code changes to CCDFGF have been made since the migration to the Solaris system. The codes PRECCDFGF version 2.01 and CCDFGF version 7.03 were used for the CRA19 analysis. The baseline version of the CCDFGF code has changed from CRA-2014 which allows for a more flexible method of modeling drilling intrusions into panels with regard to repository configuration in accordance with the APCS approach (WIPP PA 2010, Kirchner et al. 2015). A description of the conceptual approach to this change is discussed in Section 2.2.

This page intentionally left blank.

2.0 CONCEPTUAL APPROACH FOR THE CRA-2019

CCDFGF is used to assemble results obtained from calculations performed with a number of different models (e.g., BRAGFLO, PANEL, NUTS, SECOTP2D, CUTTINGS_S, and EPAUNI) to produce complementary cumulative distribution functions (CCDFs), as specified in 40 CFR 191. To produce the CCDFs, CCDFGF simulates the drilling of boreholes at the surface of the repository. Drilling location, depth (determining whether the brine pocket is penetrated) and the type of plugging pattern are treated as stochastic parameters, necessitating the simulation of many possible realizations, or futures, in order to characterize the aleatory uncertainty of the results. If the model results were free from uncertainty then the CCDF of the potential releases from the repository produced by this method would characterize the uncertainty in the releases due to the uncertainty of intrusion of the repository in the future, i.e. to the CCDF specified in 40 CFR 191. However, there is also uncertainty associated with the model results due to the lack of precise knowledge about the values of the parameters used in the models; i.e., the epistemic uncertainty. Therefore, CCDFGF also incorporates into its estimate of the total uncertainty in the results this epistemic uncertainty. CCDFGF incorporates the epistemic uncertainty by repeating the computation of results for a set of futures for each of a series of observations, or vectors, of the input data obtained from the various models. Each vector of input data is the result of a simulation in which the parameters of the model were sampled from distributions representing the epistemic uncertainty in their values. Thus, for each vector of input data CCDFGF generates one CCDF for each output variable describing the probability of the output variable taking on various values. It is the set of CCDFs for the releases that characterizes the confidence with which the location of the CCDF of releases can be estimated.

2.1 Use of DBR Scenarios in CCDFGF

The CCDFGF code calculates releases for hypothetical futures that are populated with drilling intrusion events. A typical PA analysis consists of 300 vectors, each of which has 10,000 hypothetical futures. In these futures, drilling intrusions may intersect any waste panel at any time beginning at 100 years after repository closure and may intersect a waste panel multiple times. CCDFGF calculates DBR releases from each intrusion event by translating and interpolating DBR volumes calculated at a few points in time for a much smaller set of scenarios (Table 5). For instance, while CCDFGF models intrusions into any of the ten panels, BRAGFLO_DBR simulations model intrusion events in only three of the ten panels (Panels 3, 5, or 10), and furthermore the BRAGFLO_DBR simulations select their initial conditions from a set of BRAGFLO scenarios (Table 4) in which only a single panel (Panel 5, the WP in the BRAGFLO grid) is intruded (or is undisturbed). Thus, panel lumping and abstraction also enter the CCDFGF calculations, but in terms of the combinatorial problem of what panel was intruded and to which panel(s) it is adjacent.

Table 4 – BRAGFLO Scenarios

Fundamental Scenario	Specific Scenario	Time of Drilling Intrusion(s)
E0: no drilling intrusions.	S1-BF	N/A
E1: single intrusion through an excavated area of the repository that penetrates pressurized brine in the Castile	S2-BF	350 years
	S3-BF	1,000 years
E2: single intrusion through an excavated area of the repository that does not penetrate pressurized brine in the Castile.	S4-BF	350 years
	S5-BF	1,000 years
E2E1: two intrusions into the same waste panel, the first being an E2 intrusion and the second being an E1 intrusion.	S6-BF	1,000 years for E2 intrusion 2,000 years for E1 intrusion

Each BRAGFLO_DBR scenario described in Table 5 consists of three pieces of information about the BRAGFLO_DBR simulation: (1) the initial conditions of the BRAGFLO_DBR simulation, (2) which panel is intruded during the simulation, and (3) the time of the intrusion. The initial conditions are taken from BRAGFLO simulation output from different BRAGFLO scenarios - S1-DBR selects its initial conditions from the BRAGFLO S1-BF (E0 undisturbed) scenario, while scenarios S2-DBR through S5-DBR select their initial conditions from BRAGFLO scenarios S2-BF through S5-BF (in which the WP has been previously intruded - this is the “initial” intrusion that is referred to in Table 5). The panel intruded in the BRAGFLO_DBR simulation is labeled as lower, middle, and upper, or same, adjacent, and nonadjacent, and in both cases corresponds to Panels 5, 3, and 10, respectively. The terms same, adjacent, and nonadjacent refer to the position of the intruded panel with respect to Panel 5, the WP. Lastly, the time of the intrusion specifies the time at which the initial conditions are selected from the corresponding BRAGLO scenario simulation. Thus, for BRAGFLO_DBR scenarios S2-DBR through S5-DBR (Table 5), three cases are run at each of the five intrusion times: Lower (L), Middle (M), and Upper (U). The L case corresponds to a first intrusion in Panel 5 followed by a subsequent intrusion in Panel 5. The M case corresponds to a first intrusion in Panel 5 followed by a subsequent intrusion in Panel 3. The U case corresponds to a first intrusion in Panel 5 followed by a subsequent intrusion in Panel 10.

Table 5 – BRAGFLO-DBR Scenarios

Scenario	Description
S1-DBR	*Initially undisturbed repository (i.e., E0 conditions).* Intrusion into lower, middle, or upper waste panel at 100; 350; 1,000; 3,000; 5,000; or 10,000 years: 18 combinations.
S2-DBR	Initial E1 intrusion at 350 years followed by a second intrusion into the same, adjacent, or nonadjacent waste panel at 550; 750; 2,000; 4,000; or 10,000 years: 15 combinations.
S3-DBR	Initial E1 intrusion at 1,000 years followed by a second intrusion into the same, adjacent, or nonadjacent waste panel at 1,200; 1,400; 3,000; 5,000; or 10,000 years: 15 combinations.
S4-DBR	Initial E2 intrusion at 350 years followed by a second intrusion into the same, adjacent, or nonadjacent waste panel at 550; 750; 2,000; 4,000; or 10,000 years: 15 combinations.
S5-DBR	Initial E2 intrusion at 1,000 years followed by a second intrusion into the same, adjacent, or nonadjacent waste panel at 1,200; 1,400; 3,000; 5,000; or 10,000 years: 15 combinations.

The BRAGFLO_DBR L case is then used by CCDFGF to represent a drilling intrusion event in a future in which the same panel has been previously intruded (the "Same" case in CCDFGF). For example, if an intrusion in Panel 10 followed a previous intrusion into Panel 10, then results from the L case (which were calculated for the more conservative case in which Panel 5 is intruded twice) would be used.

The BRAGFLO_DBR M case is used by CCDFGF to represent a drilling intrusion event in a future in which the most recently intruded panel was adjacent to the panel currently being intruded (the "Adjacent" case in CCDFGF). For example, if an intrusion in Panel 10 followed a previous intrusion into Panel 8 (which is adjacent to Panel 10; see Section 2.2 below), then the M case results (which were actually calculated for the more conservative case in which Panel 3 is intruded after Panel 5) would be used.

The BRAGFLO_DBR U case is used by CCDFGF to represent a drilling intrusion event in a future in which the most recently intruded panel was non-adjacent to the panel currently being intruded (the "Nonadjacent" case in CCDFGF). For example, if an intrusion in Panel 10 followed a previous intrusion into Panel 3 (which is not adjacent to Panel 10; see Section 2.2 below), then the U case results (which were actually calculated for the more conservative case in which Panel 10 is intruded after Panel 5) would be used.

2.2 Redefinition of Panel Adjacency in CCDFGF

Version 6.02 (and previous versions) of the CCDFGF code specified 144 model node locations for drilling intrusions, which corresponded to 14 locations per panel for Panels 1-8 and 16 locations each for Panels 9 and 10 (Figure PA-11 in Appendix PA, 2014). For a given intrusion into the repository, a node was chosen at random with equal probability. Node-to-Panel correlations and "panel adjacency" (the adjacent or non-adjacent relationship between panels) were specified explicitly in the CCDFGF code (i.e., were "hard-coded"). As explained above, panel adjacency is relevant to the calculation of DBRs. The CCDFGF code version 6.0 was used in CRA-2014 PA calculations.

Beginning with CCDFGF v. 7.00, the use of 144 node locations for intrusions was replaced with the use of 10 node locations (each corresponding directly to a specific panel), with node probabilities specified at run-time via relative panel areas in the CCDFGF control file (WIPP PA 2010). Panel adjacency is handled by specifying immediate (i.e., adjacent) neighbors for each panel in the CCDFGF control file.

Panel neighbor relationships were modified in the APCS approach to correspond to the degree of separation by panel closures instead of merely spatial proximity. The modification is consistent with the definition that panels having one or fewer panel closures between them are considered neighbors and is summarized in Table 6. Some conservativity with respect to releases is built into this approach as a result of the reconsideration of panel adjacencies following intrusions. This approach also accommodates the removal of panel closures in the south (Zeitler and Day (2017) and Zeitler et al. (2017)).

Table 6 – Listing of Adjacent Panel Relationships for CRA-2014 and CRA-2019 PAs

Panel	CRA-2014 PA	CRA-2019 PA
1	2, 10	10
2	1, 3, 10	10
3	2, 4, 9	4, 5, 6, 9, 10
4	3, 9	3, 5, 6, 9, 10
5	6, 9	3, 4, 6, 9, 10
6	5, 7, 9	3, 4, 5, 9, 10
7	6, 8, 10	10
8	7, 10	10
9	3, 4, 5, 6, 10	3, 4, 5, 6, 10
10	1, 2, 7, 8, 9	1, 2, 3, 4, 5, 6, 7, 8, 9

3.0 CCDFGF METHODOLOGY

The performance assessment methodology accommodates both aleatory (i.e., stochastic) and epistemic (i.e., subjective) uncertainty in its constituent models. Aleatory uncertainty pertains to unknowable future events such as intrusion times and locations that may affect repository performance. It is accounted for by the generation of random sequences of future events. Epistemic uncertainty concerns parameter values that are assumed to be constants and the constants' true values are uncertain due to a lack of knowledge about the system. An example of a parameter with epistemic uncertainty is the permeability of a material. Epistemic uncertainty is accounted for by sampling of parameter values from assigned distributions. One set of sampled values required to run a WIPP PA calculation is termed a vector. The performance assessment models are executed for three replicates of 100 vectors, each vector being a realization resulting from a particular set of parameter values. A sample size of 10,000 possible sequences of future events is used in the calculations to estimate an exceedance probability of 0.001 (Helton et al. 1998). The releases for each of 10,000 possible sequences of future events are tabulated for each of the 300 vectors, totaling 3,000,000 possible sequences.

For a random variable, the complementary cumulative distribution function (CCDF) provides the probability of the variable being greater than a particular value. By regulation, performance assessment results are presented as a distribution of CCDFs of releases (U.S. EPA 1996). Each individual CCDF summarizes the likelihood of releases across all futures for one vector of parameter values. The uncertainty in parameter values results in a distribution of CCDFs.

The overall mean CCDF is computed as the arithmetic mean of the three mean CCDFs from each replicate. Confidence limits are computed about the overall mean CCDF using the Student's t-distribution, the mean CCDFs from each replicate, and the standard error based on the three replicate means. The four release mechanisms that are considered in this report include cuttings and cavings, spallings, direct brine releases, and transport releases. Cuttings and cavings and spallings releases determine the quantity of solid waste brought to the surface as a result of a drilling intrusion through a waste panel (Kicker 2019a). Direct brine releases occur when the WIPP repository is penetrated by a borehole while under conditions of sufficient brine pressure and saturation, causing the brine to migrate up through the intruding borehole to reach the land surface (Bethune 2019a, Day 2019b), and transport releases occur if brine flows through a borehole to the Culebra and out to the land withdrawal boundary (Day 2019b, Sarathi 2019). Finally, total releases are calculated by summing the releases across each potential release pathway, namely cuttings and cavings releases, spallings releases, direct brine releases, and transport releases.

3.1 Random Seed in the CCDFGF Control Files

One of the features that the CCDFGF control file initializes is the random number generator in the code. Setting the random number seed in the control file determines the sequence of pseudo random numbers used by CCDFGF. This sequence of numbers affects several stochastic parameters, such as the drilling location, depth, and type of plugging pattern, utilized when CCDFGF simulates the drilling of boreholes at the surface of the WIPP repository.

For the CRA-2019 PA, the same random seeds for CCDFGF were used as in the CRA-2014 PA. This was done to allow a vector by vector comparison of the results of the CRA-2014 PA to those obtained in the CRA-2019 PA. As the random seeds used to initialize the sampling of the epistemic parameters were unchanged in the CRA-2014 PA and the CRA-2019 PA, any differences between the analyses can be attributed solely to the changes in the parameters, modeled processes, and repository reconfiguration and not the random seed choice. Random seeds used in the CRA-2019 PA calculations are specified in the files ccgf_CRA19_control_r*n*.inp, where *n* = 1,2,3.

3.2 Run Control

A full description of the run control for the CRA19 analysis, including names and locations of input and output files, can be found in Long (2019). As outlined in AP-181 (Zeitler 2019c), in cases where comparisons are made to the CRA-2014 PA results, the CRA14 (Rev. 2) results from the Solaris migration integration tests are used (Kirchner et al. 2014, Kirchner et al. 2015).

4.0 RESULTS

Results of the CRA-2019 PA calculations are described in subsections for each release component. Mean CCDFs for each release pathway were calculated for three replicates in the CRA19 analysis, as well as the 95% confidence limit on the mean. At the end of each subsection, results of the CRA-2019 PA are compared to those found in the CRA-2014 PA.

Normalized releases for cuttings and cavings are discussed in Subsection 4.1, spallings releases are presented in Subsection 4.2, direct brine releases are discussed in Subsection 4.3, and normalized transport releases are presented in Subsection 4.4. Finally, total normalized releases are shown in Subsection 4.5. In the results that follow, summary statistics and plots were generated with Python, an open-source software package. All plotted data were read from the WIPP PA Results Database (PA_Results).

4.1 Cuttings and Cavings Normalized Releases

CRA-2019 PA cuttings and cavings releases are presented in this section and compared to results obtained in the CRA-2014 PA. Cuttings and cavings releases depend on cuttings and cavings volumes and sampled waste stream concentrations. The assumed cuttings and cavings concentration for a given intrusion is based on waste stream volumes (which determine the probability of selecting a given waste stream) as well as waste stream concentrations over time. A listing of the 10 radionuclides that are included in CCDFGF calculations and their respective inventory quantities are discussed in Kicker (2019b).

Figure 1, Figure 2, and Figure 3 show the CRA-2019 PA cuttings and cavings release CCDFs for replicates 1, 2, and 3, respectively, while Figure 4 shows the 95 percent confidence limits about the overall cuttings and cavings mean for CRA19 and compares it to the CRA14 results. The CRA-2014 PA and the CRA-2019 PA cuttings and cavings CCDFs for the overall release volumes are plotted together in Figure 5.

The CRA-2019 PA approach to calculating cuttings and cavings remains the same as the CRA-2014 PA approach. Cavings volumes are combined with sampled inventory concentrations to determine releases for a single intrusion; the number of intrusions for a given future is impacted by the drilling rate. As discussed in Kicker (2019a), the only change in CUTTINGS_S that impacts cuttings and cavings releases is an adjustment to the lower bound of the parameter BOREHOLE:TAUFAIL, which had negligible impact on the cuttings and cavings volume results. As discussed in Kicker (2019b), while higher activities are shown for the CRA19 inventory compared to CRA14 inventory, the activities in EPA units are nearly identical compared to the CRA14 inventory due to the normalization process of converting Ci to EPA units, and the inventory changes do not significantly impact direct solids releases for CRA-2019 PA calculations. Therefore, the modest increase in cuttings and cavings releases from CRA-2014 to CRA-2019 can be mainly attributed to the increased drilling rate.

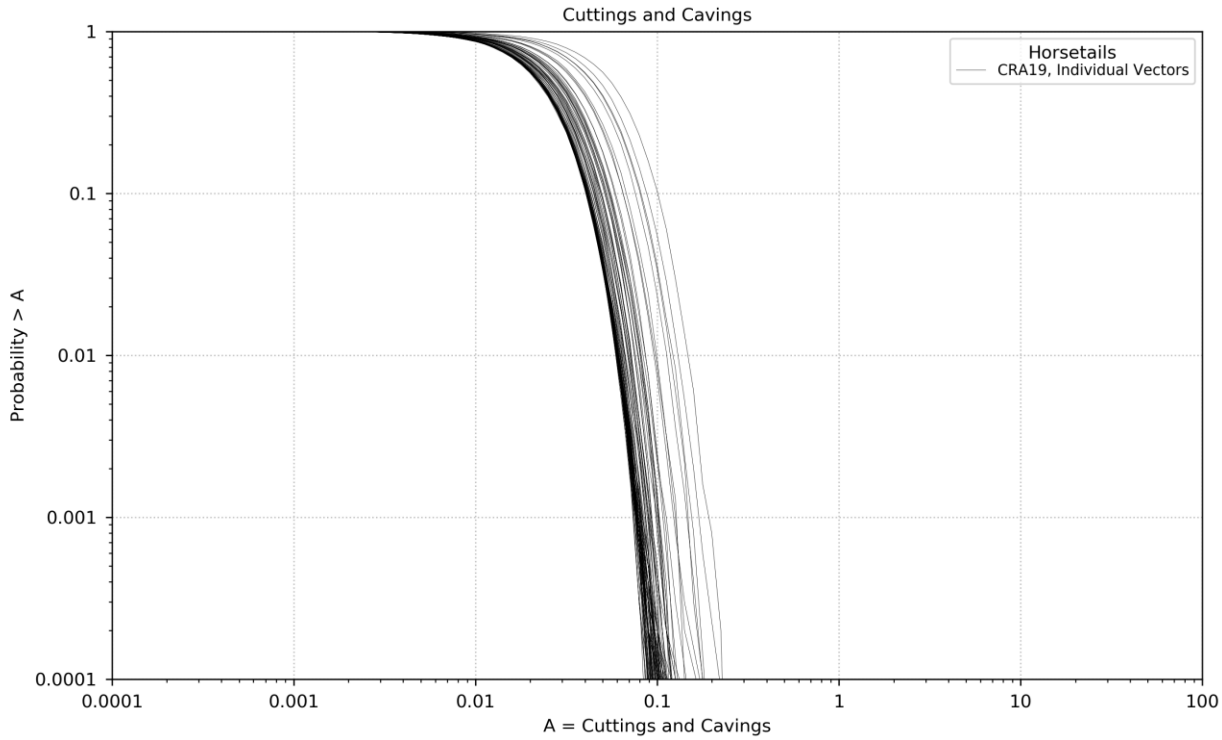

Figure 1 – Replicate 1 Cuttings and Cavings Normalized Releases

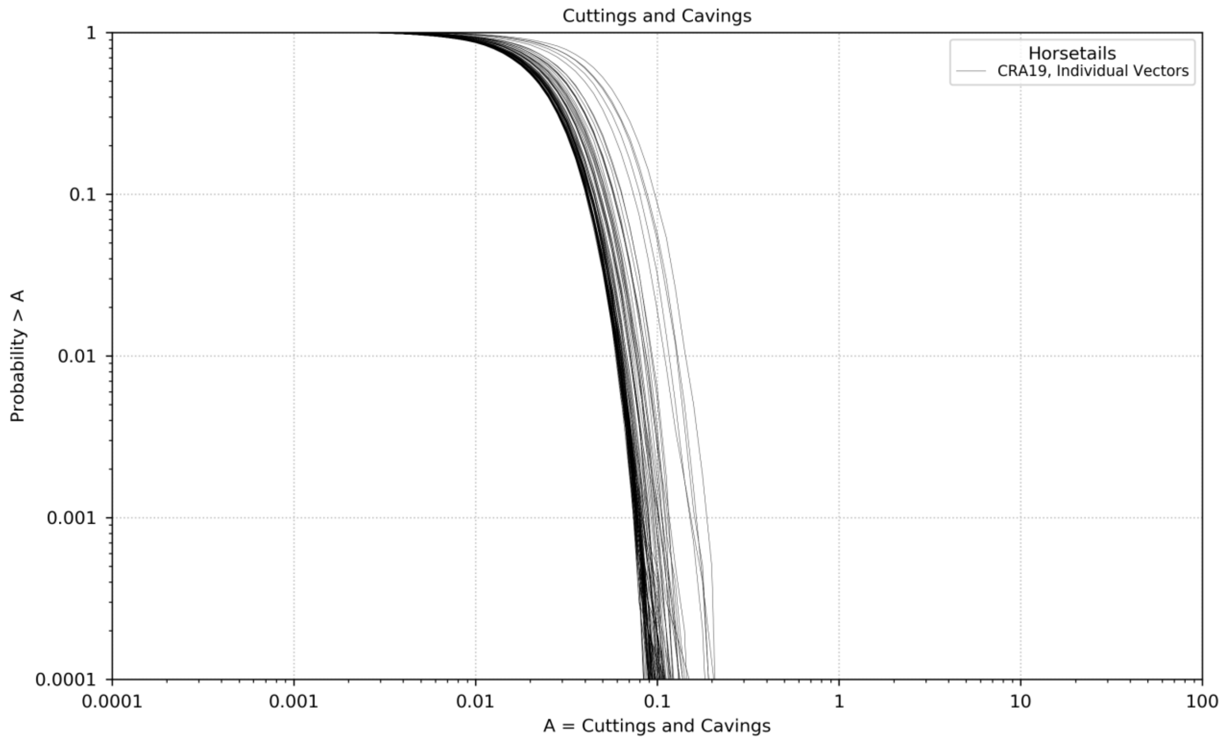

Figure 2 – Replicate 2 Cuttings and Cavings Normalized Releases

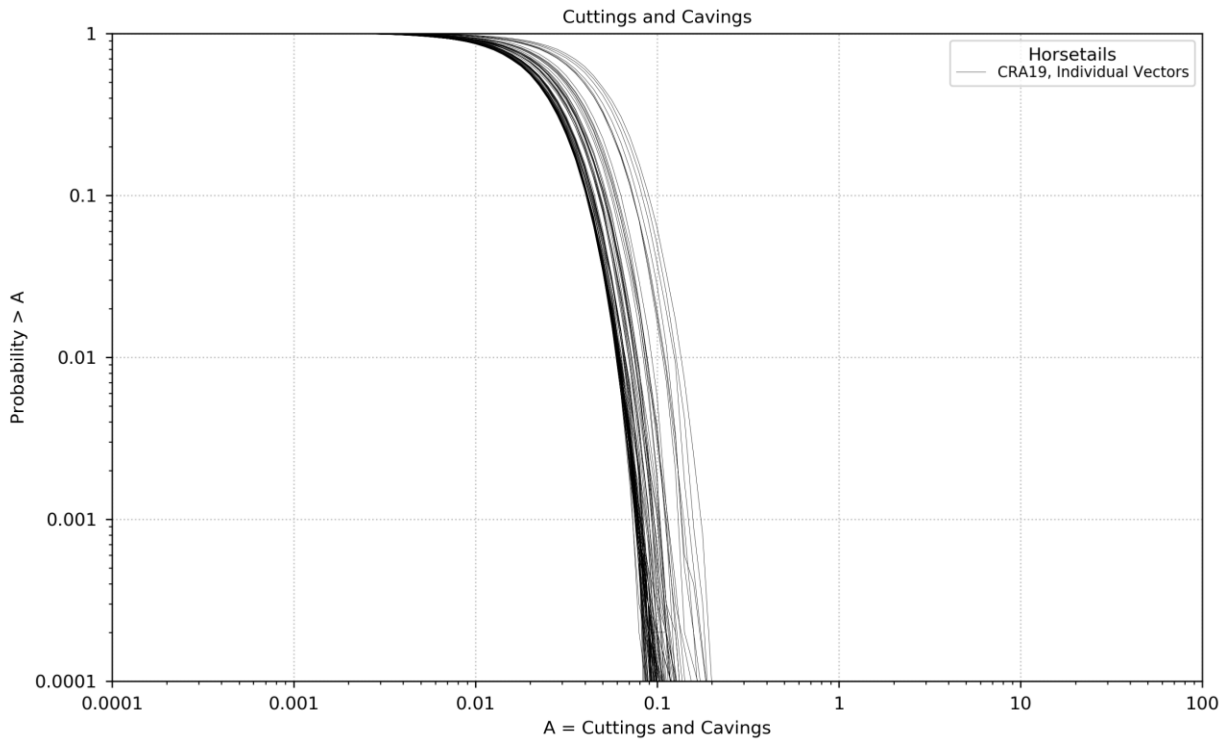

Figure 3 – Replicate 3 Cuttings and Cavings Normalized Releases

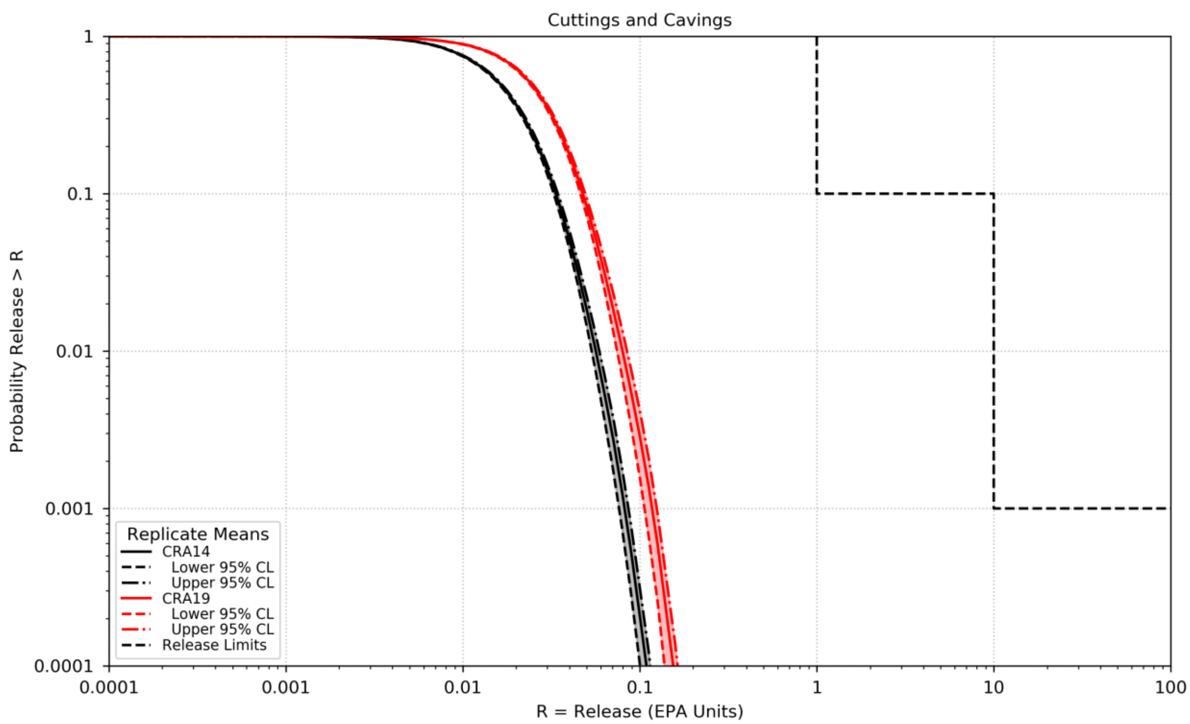

Figure 4 – Confidence Limits on Overall Mean for Cuttings and Cavings Releases

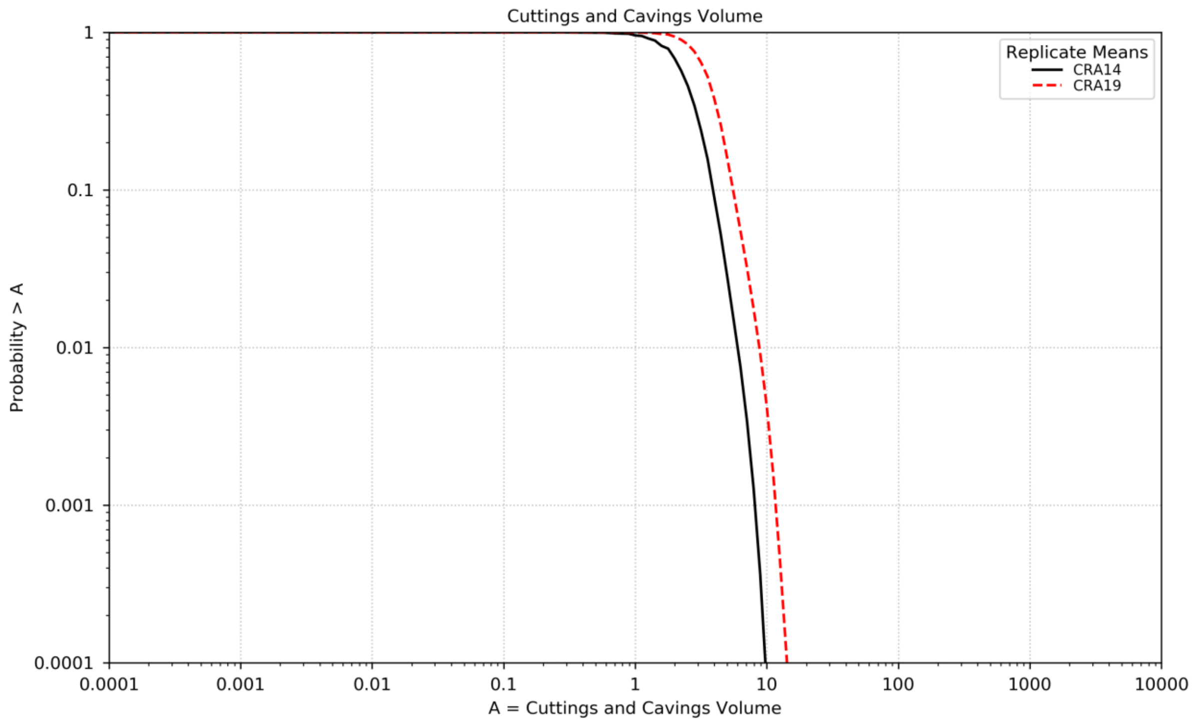

Figure 5 – Overall Mean CCDFs for Cuttings and Cavings Release Volumes

4.2 Spallings Normalized Releases

CRA-2019 PA spallings releases are presented in this section and compared to results obtained in the CRA-2014 PA. Figure 6, Figure 7, and Figure 8 show the CRA-2019 PA spallings release CCDFs for replicates 1, 2, and 3, respectively. Figure 9 shows the 95 percent confidence limits about the overall spallings mean for CRA-2019 PA compared to CRA-2014 PA. Figure 10 compares the overall mean CCDFs for the spallings volumes results of the two analyses.

As discussed in Section 1.1.16, an updated version of DRSPALL is used in the CRA-2019 PA, which corrects an error found in previous versions. In accordance with the planning document (Zeitler 2019c), the CRA-2019 PA calculations are compared to CRA-2014 Rev. 2 results, which have been rerun on the Solaris system with this updated version of DRSPALL (Kicker 2019a). Therefore, the differences between spallings results in the plots shown here are not due to the correction of the code error.

Spallings releases are calculated from spallings volumes and spallings concentrations but are also affected by changes to both the drilling rate and the plugging pattern (which in part determines the type of intrusion (e.g., E0, E1, E2) and thus which repository pressure history is accessed). The increased drilling rate leads to increased spallings releases due to more intrusions and the increased mean value of PBRINE leads to increased spallings releases due to an increased probability of relatively high-pressure E1 intrusions; however the plugging pattern changes resulted in a decrease in spallings releases due to a decreased probability of E1 and E2 intrusions

(Section 1.1.11). While these changes are independently relatively impactful, they counteract each other to some degree resulting in a smaller change overall.

Spallings concentrations are calculated as the waste stream volume-averaged concentration of contact-handled waste. The levels of activity (in EPA units) in the CRA19 analysis are similar to those in the CRA14 analysis, resulting in similar levels of spallings concentrations (Kicker 2019b). However, several model changes made since CRA-2014 have led to increased average waste panel pressures for all waste panel areas and most BRAGFLO scenarios. These changes include adaption of the APCS approach, the addition of brine radiolysis in the gas generation process, and the refinement to the steel corrosion rates. Since spallings releases are a function of repository pressure at the time of intrusion, increases in pressure necessarily translate to increased spallings release volumes. The increased spallings volumes combined with steady concentration levels lead to an increase in spallings releases. An in-depth discussion of these changes and their effect on repository pressures and spallings volume releases are discussed in detail in Day (2019b) and Kicker (2019a).

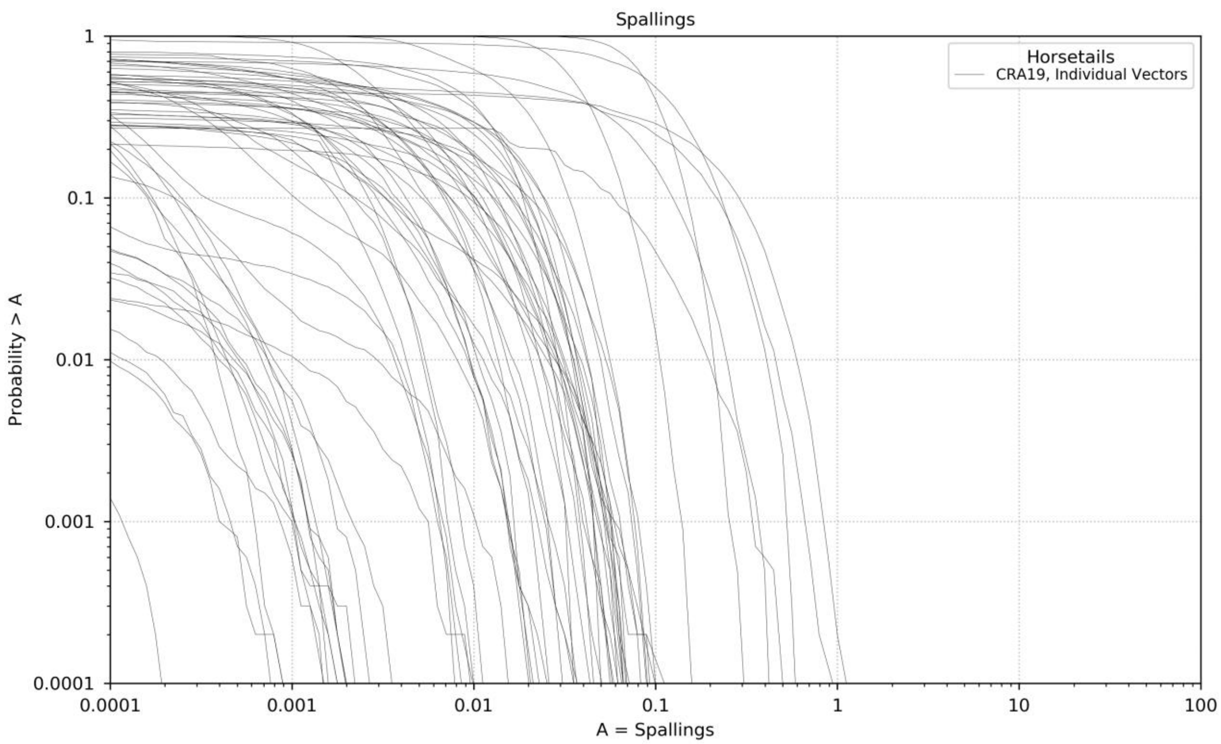

Figure 6 – Replicate 1 Spallings Normalized Releases

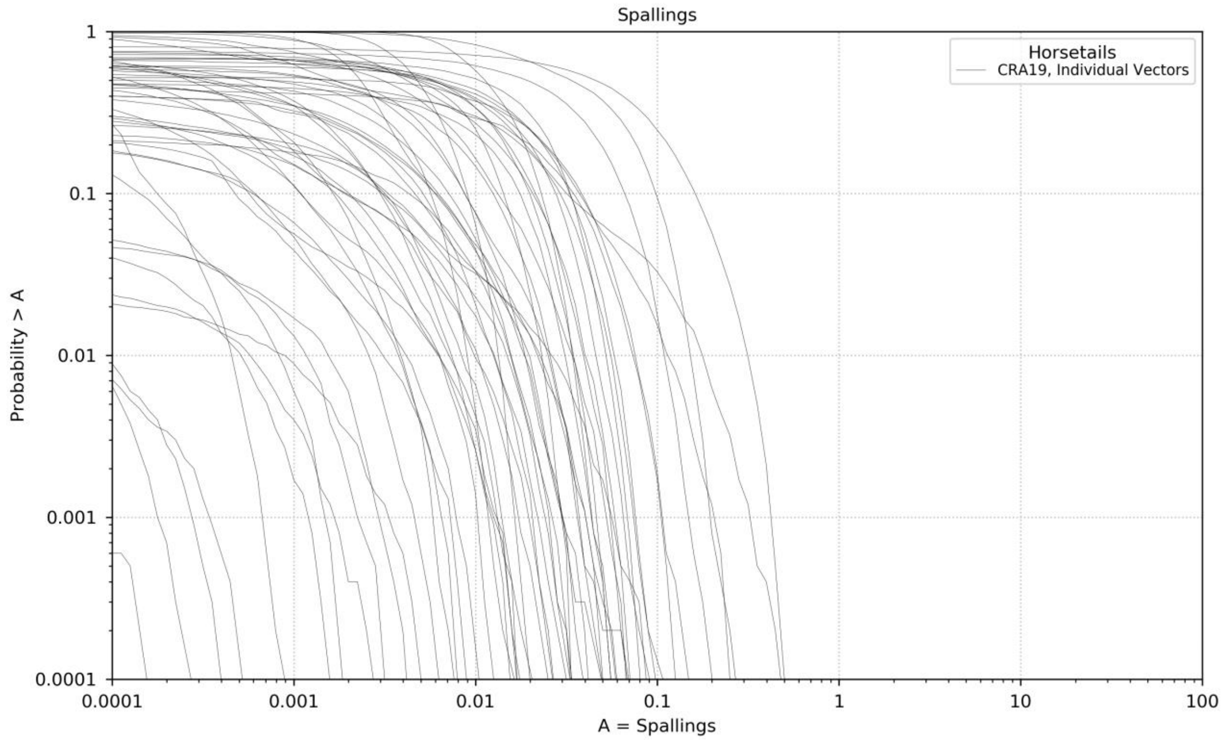

Figure 7 – Replicate 2 Spallings Normalized Releases

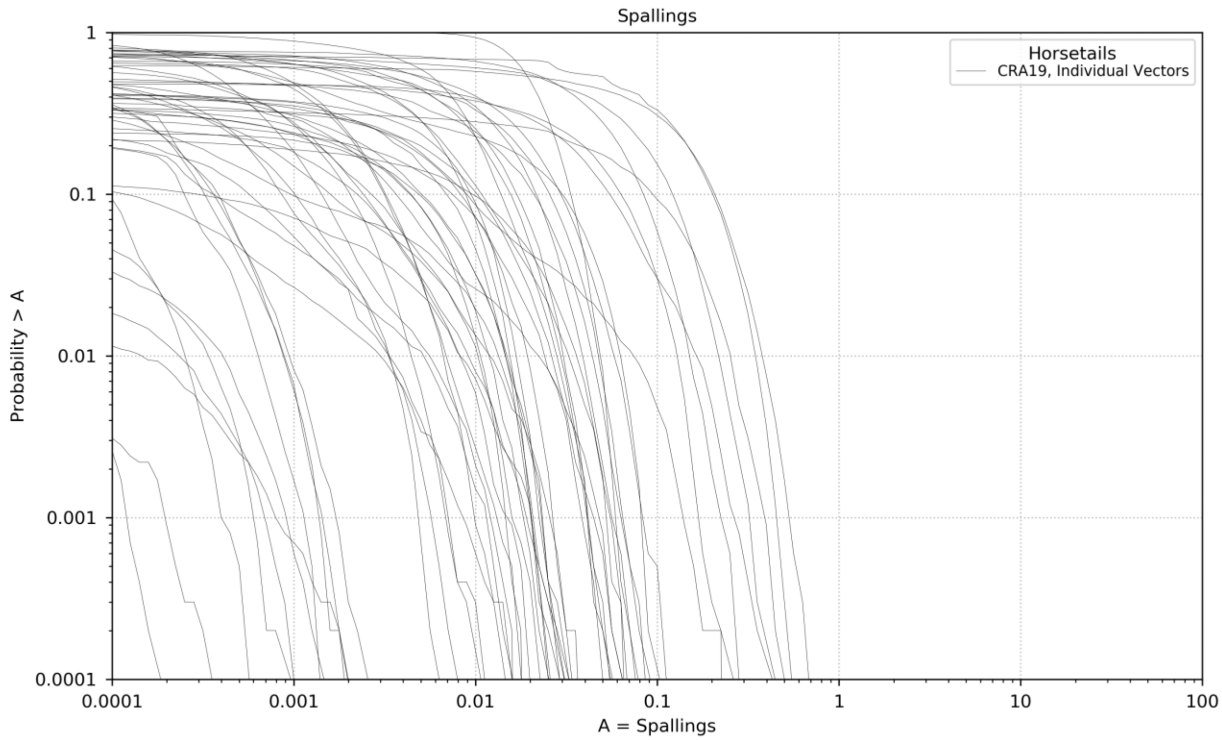

Figure 8 – Replicate 3 Spallings Normalized Releases

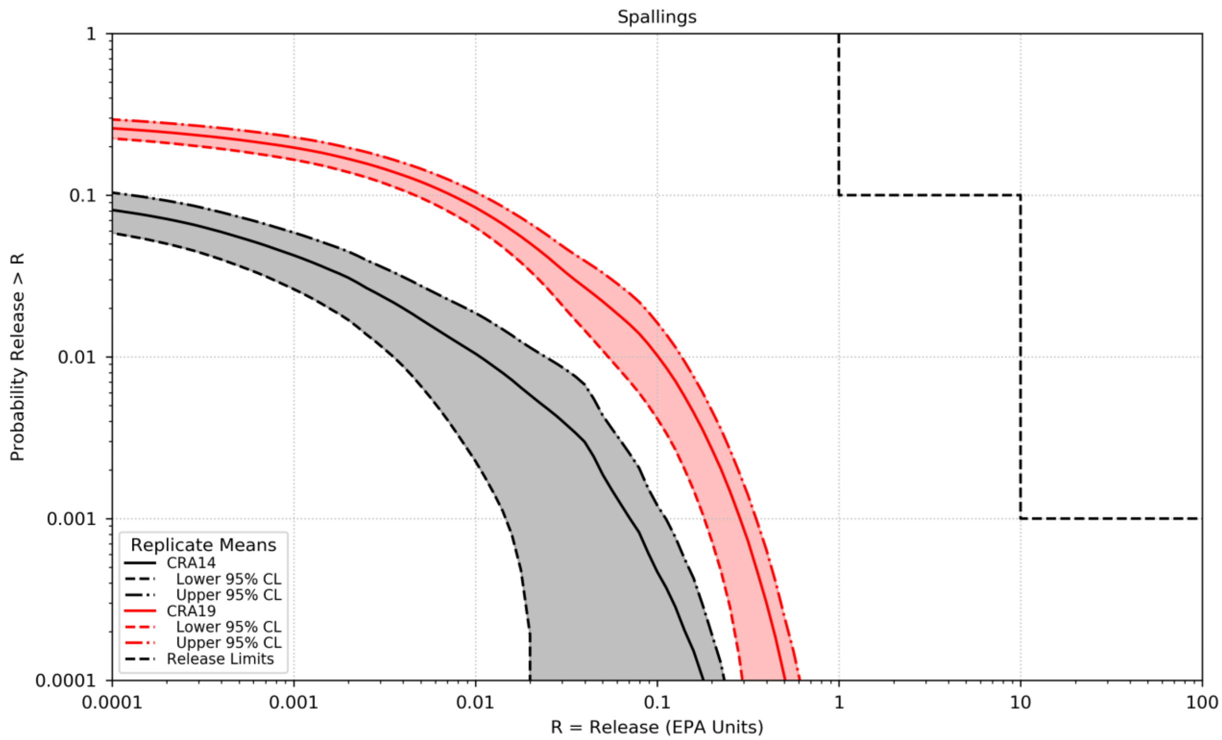

Figure 9 – Confidence Limits on Overall Mean for Normalized Spallings Releases

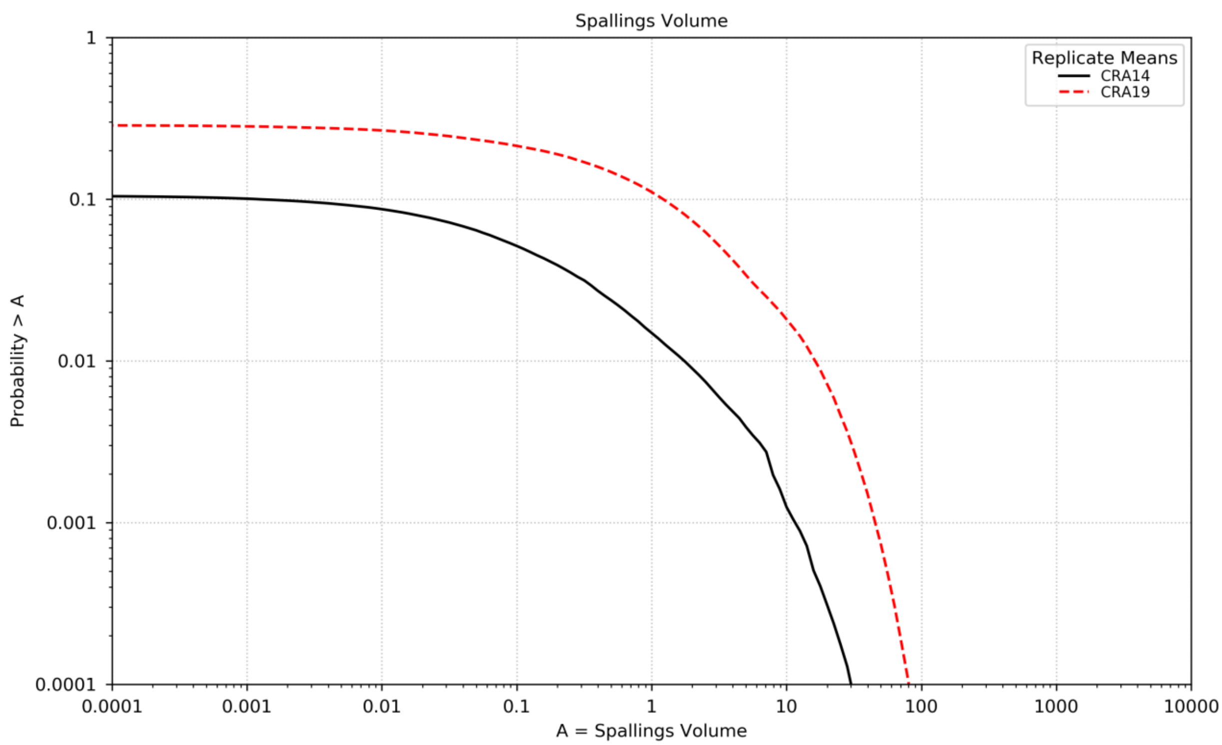

Figure 10 – Overall Mean CCDFs for Spallings Volumes

4.3 Normalized Direct Brine Releases

CRA-2019 PA normalized direct brine releases (DBRs) are presented in this section and compared to results obtained in the CRA-2014 PA. Figure 11, Figure 12, and Figure 13 show the normalized CRA-2019 PA CCDFs for direct brine releases in replicates 1, 2, and 3, respectively. Figure 14 shows the 95 percent confidence limits about the DBR overall mean, comparing CRA-2019 PA results to those from CRA-2014 PA. The CRA-2014 PA and the CRA-2019 PA CCDFs for the mean DBR volumes are plotted together in Figure 15.

DBRs are calculated from DBR volumes and mobilized actinide concentrations in brine but are also affected by changes to both the drilling rate and the plugging pattern (which determines the type of intrusion (e.g., E0, E1, E2) and thus which repository pressure/saturation history is accessed). The increased drilling rate leads to increased DBRs due to more intrusions and the increased mean value of PBRINE leads to increased spallings releases due to an increased probability of relatively high-pressure E1 intrusions; however the plugging pattern changes resulted in a decrease in spallings releases due to a decreased probability of E1 and E2 intrusions (Section 1.1.11). While these changes are independently relatively impactful, they counteract each other to some degree resulting in a smaller change overall.

This analysis shows that the average and maximum DBR volumes from the CRA-2019 PA are substantially higher than those from the CRA-2014 PA. As discussed in Bethune (2019a) and Day (2019b), the primary impacts of changes are substantially increased brine pressures for E1 intrusion scenarios (corresponding to S2-BF and S3-BF from Table 4 and S2-DBR and S3-DBR from Table 5), E2E1 intrusion scenarios (corresponding to S6-BF from Table 4), and substantially higher saturations in the middle intrusion locations. These observed differences are influenced by increased total gas generation due to the availability of brine within the waste panel and south rest-of-repository that flows from the Castile brine reservoir, up the intrusion borehole, to the waste panel, and across the abandoned panel closure area to the south rest-of-repository. These changes to DBR volumes appear to be driven by differences in the initial conditions derived from the BRAGFLO Salado model, particularly those that create increased brine pressure in the lower intrusion region, and increased brine pressure and saturation in the middle intrusion region.

As discussed in Sarathi (2019), U(VI) concentrations in brine remain similar for CRA-2019. The median and mean concentrations of Am(III), Pu(III), and Pu(IV) in brine decreased, and total mobile radioactivity concentrations decreased overall. However, the increase in DBR release volumes, along with the combined impacts of drilling rate and plugging patterns, more than offset the decrease in realized radionuclide concentrations, leading to an overall increase in DBRs. See Bethune (2019a) for a more complete discussion of DBR volumes.

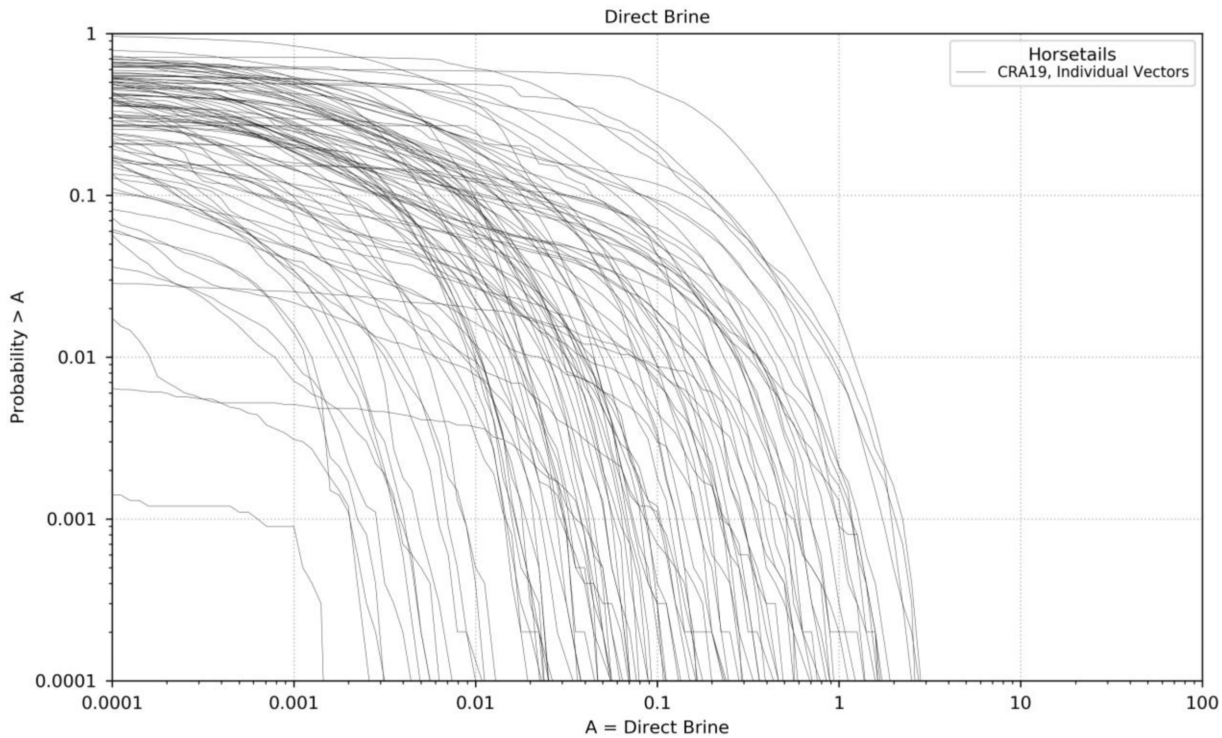

Figure 11 – Replicate 1 Direct Brine Normalized Releases

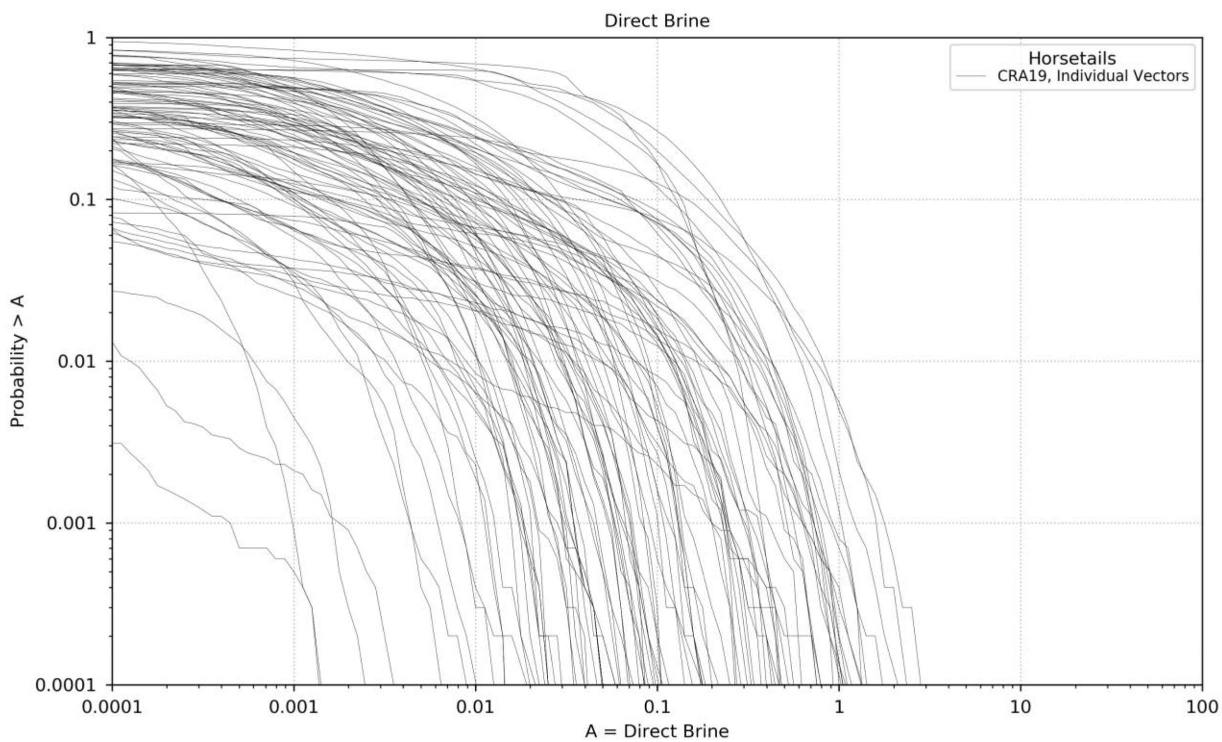

Figure 12 – Replicate 2 Direct Brine Normalized Releases

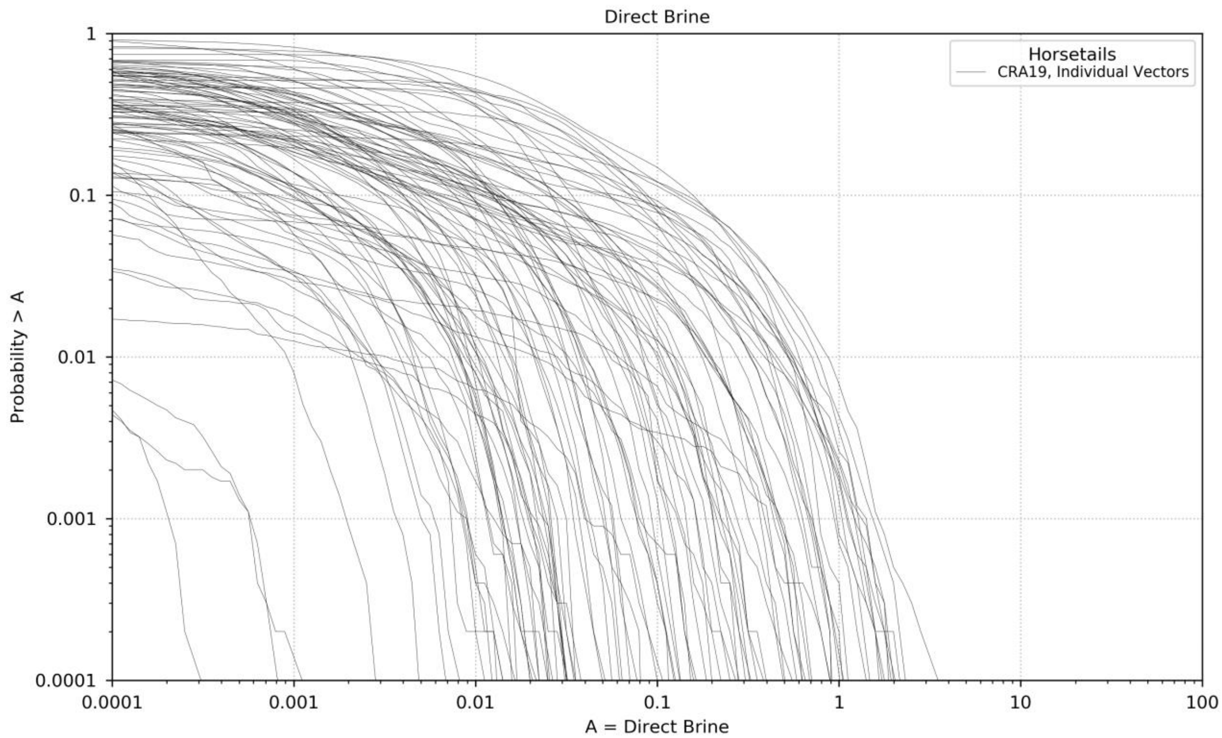

Figure 13 – Replicate 3 Direct Brine Normalized Releases

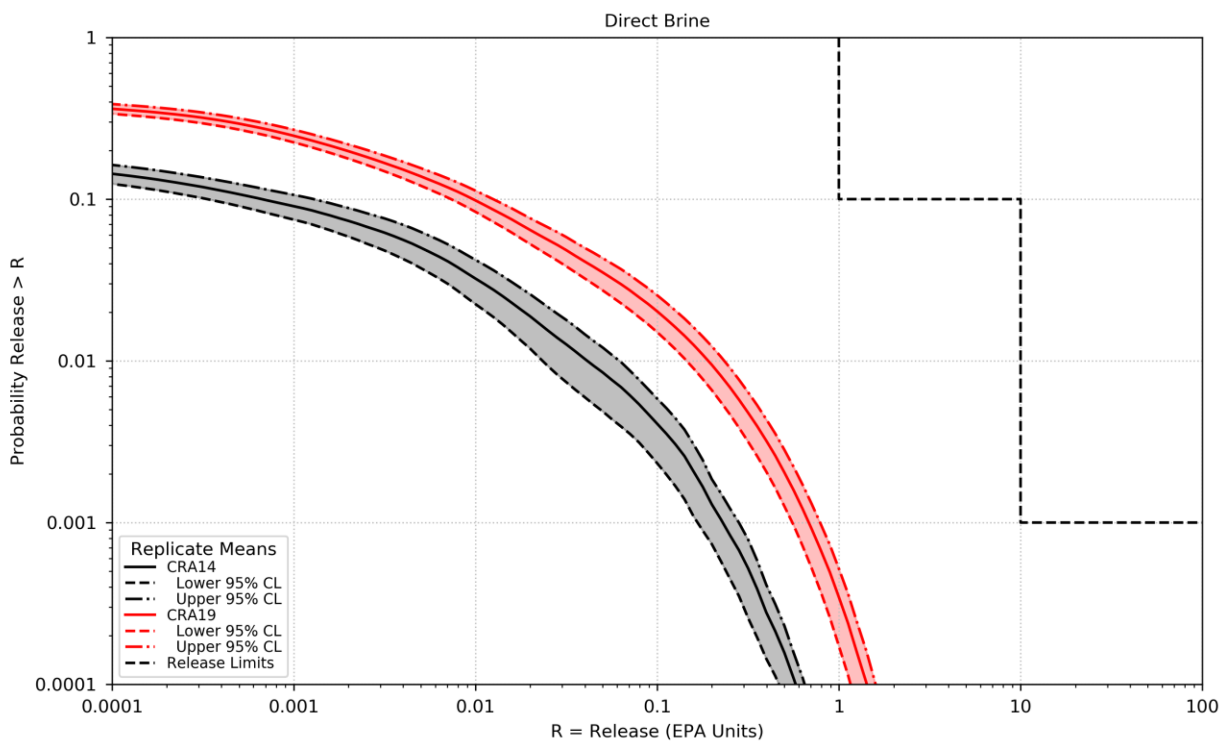

Figure 14 – Confidence Limits on Overall Mean for Normalized Direct Brine Releases

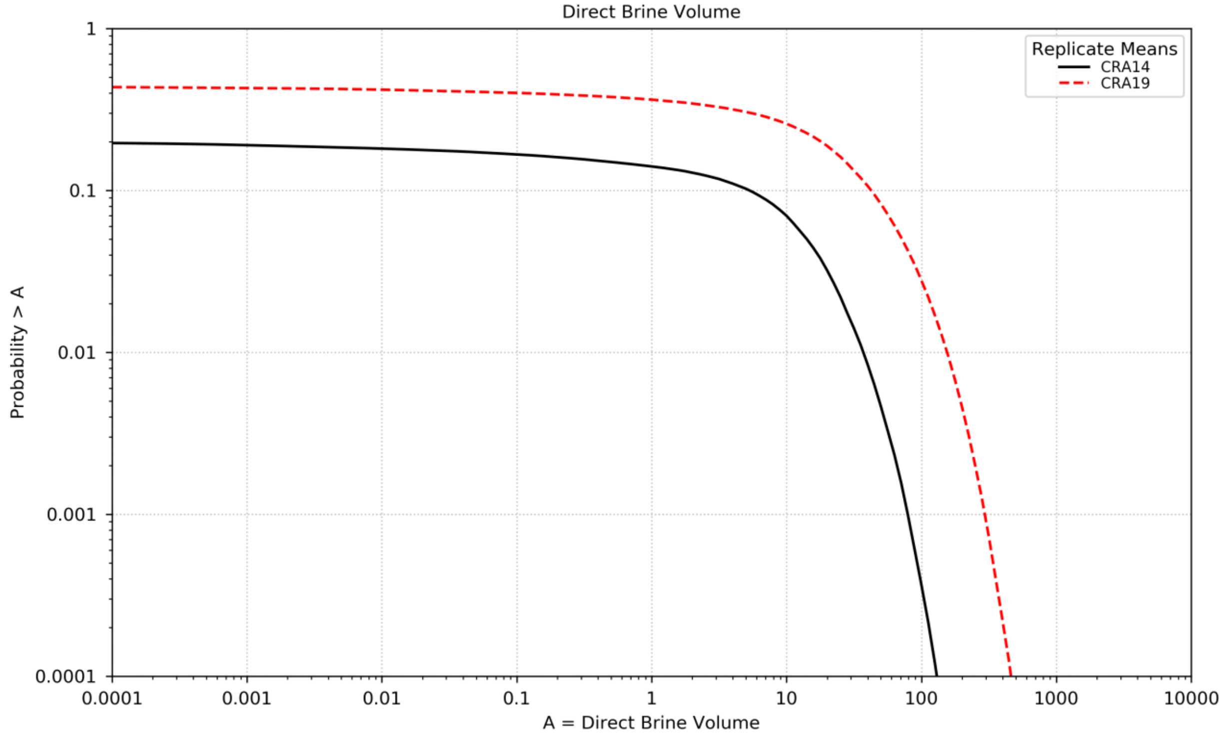

Figure 15 – Overall Mean CCDFs for Direct Brine Volumes

4.4 Normalized Transport Releases from the Culebra

CRA-2019 PA normalized transport releases from the Culebra are presented in this section and compared to results obtained in the CRA-2014 PA. Figure 16, Figure 17, and Figure 18 show the CRA-2019 PA CCDFs for Culebra releases to the land withdrawal boundary (LWB) for replicates 1, 2, and 3, respectively. It is clear from those plots that releases from the Culebra are relatively low and rare compared to releases from those mechanisms discussed above.

The cumulative discharges up the borehole are tabulated from NUTS and PANEL output and comprise the discharges to the Culebra. These are the sources for the releases from the Culebra. For BRAGFLO scenarios S1-S5 (Table 4), the radionuclide discharge through the shaft and the radionuclide discharge through the anhydrite marker beds (all three combined) to the LWB are also tabulated. As discussed in Sarathi (2019), there were no radionuclide discharges through the shaft. Similarly, the CRA-2019 results indicate no meaningful radionuclide discharges through the anhydrite marker beds across the LWB for the undisturbed scenario (S1-BF).

Transport releases through the Culebra and across the land withdrawal boundary are impacted both by the radionuclide concentration in the brine and by the amount of brine released to the Culebra (as well as drilling rate and plugging pattern for reasons mentioned above). Radionuclide concentrations are overall similar between CRA-2014 and CRA-2019, but the lumped uranium radionuclide representation (U234L) demonstrated the most substantial change on a lumped radionuclide basis (Sarathi 2019). The U234L cumulative discharges have increased due to the increase in its isotope-to-element mole fractions. This is impactful because U(VI) is assumed to have low adsorption in the Culebra, and thus is more likely to reach the

LWB in the Culebra. Figure 19 shows the mean CCDFs for releases to and from the Culebra by radionuclide for CRA-2014 (top) and CRA-2019 (bottom). One small change since the CRA-2014 is the increased contribution of Am-241 to the overall releases to the Culebra, which was previously dominated by Pu-239. Despite the releases to the Culebra being dominated by Pu-239 and Am-241, releases from the Culebra are dominated by U-234 by virtue of a partition function (K_D) parameter value used in the Culebra flow model that is approximately two orders of magnitude lower than for any other radionuclide and lower values of K_D are associated with faster transport through the Culebra.

Brine flows up the intrusion borehole obtained in CRA-2019 are increased compared to CRA-2014 PA (Day 2019b). Consequently, volumes of brine flowing up to the Culebra are increased. The changes introduced in CRA-2019 PA lead to increased waste panel pressures following intrusion into pressurized brine below the repository (as discussed in Section 4.2), which also tend to increase releases to the Culebra.

The NUTS and PANEL discharge results take into account brine flows and brine concentrations. For BRAGFLO scenarios 2, 3, and 6 (i.e., Castile brine intrusions), mean radionuclide discharges are similar to those found in CRA-2014 (Sarathi 2019). Although the median discharge has decreased, that decrease is slightly offset because high-consequence outliers have increased. While the mean brine discharges are similar for these scenarios, both the median and outlier values have decreased. In scenarios 4 and 5, the mean and outlier radionuclide discharges both see a slight decrease, while the mean and outlier brine discharges both increased slightly (Sarathi 2019).

The cumulative mass fluxes to the LWB show several instances with unphysical negative cumulative releases, ranging from -1.08e-4 kg to less than -1e-100 kg. While most of these values are too small to have any impact on the release curves, SECOTP2D values are used as a scaling factor in CCDFGF. Therefore, it can be challenging to intuit the magnitude at which they do begin to affect releases. An analysis was performed in Bethune (2019b) to bound the unaccounted for potential releases, and determined it to have no impact at the compliance level.

The overall mean releases from and to the Culebra along with 95% confidence limits comparing CRA-2014 PA and the CRA-2019 PA are shown in Figure 20 and Figure 21, respectively. The increases in drilling rate and brine flows up the borehole lead toward increased releases to the Culebra, while the reduction in mobile radionuclide concentrations lead toward decreased releases to the Culebra. The isotopic ratio for uranium leads toward increased uranium releases to and from the Culebra. Overall, transport releases through the Culebra and across the land withdrawal boundary are slightly increased compared to results for CRA-2014 PA.

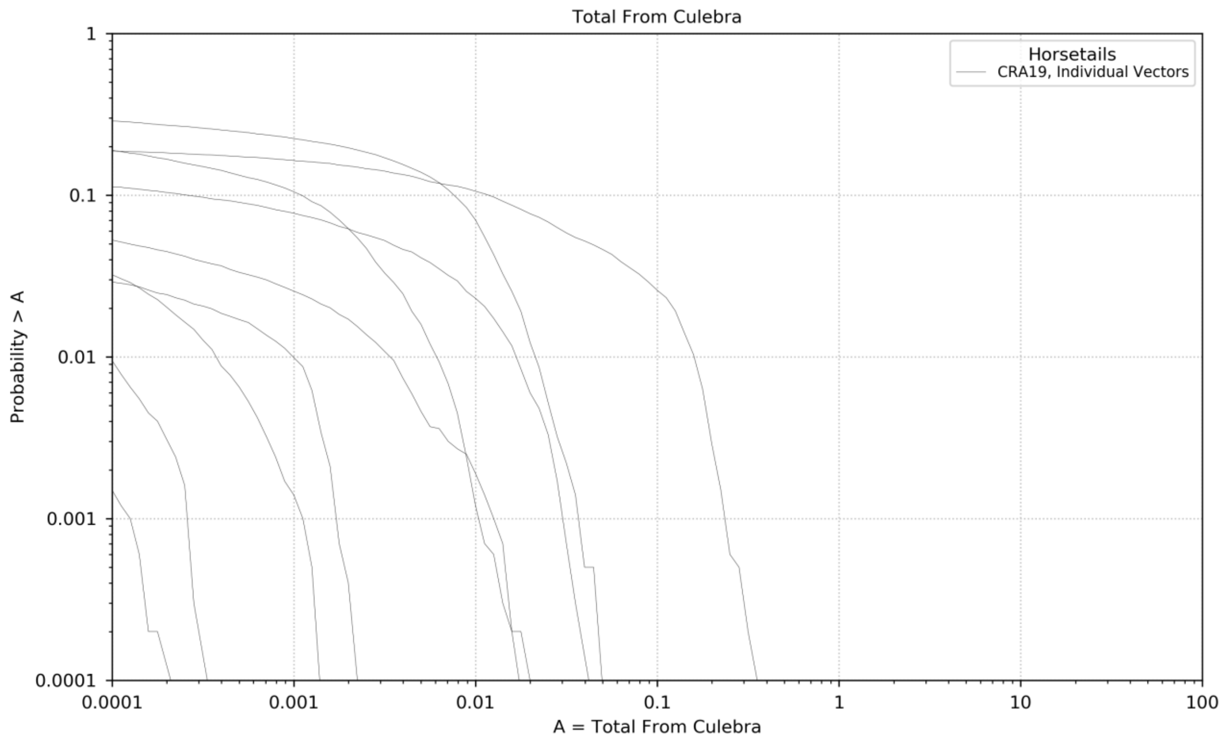

Figure 16 – Replicate 1 Normalized Culebra Transport Releases

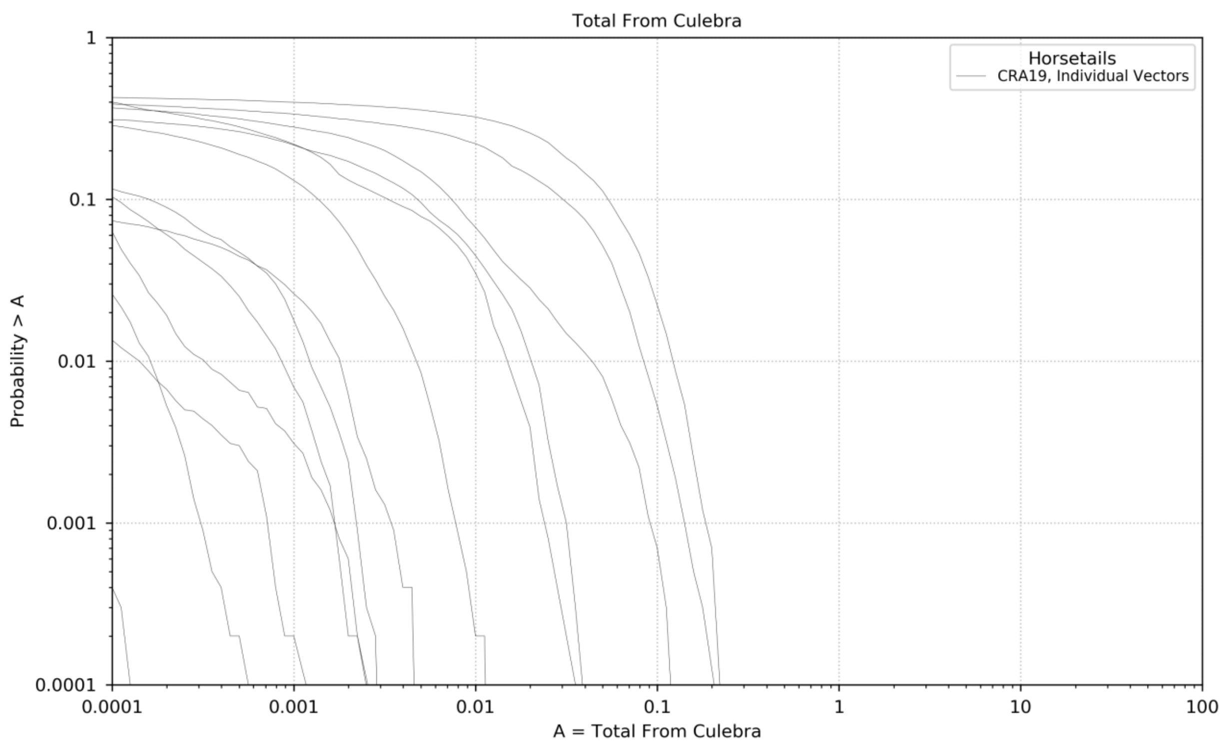

Figure 17 – Replicate 2 Normalized Culebra Transport Releases

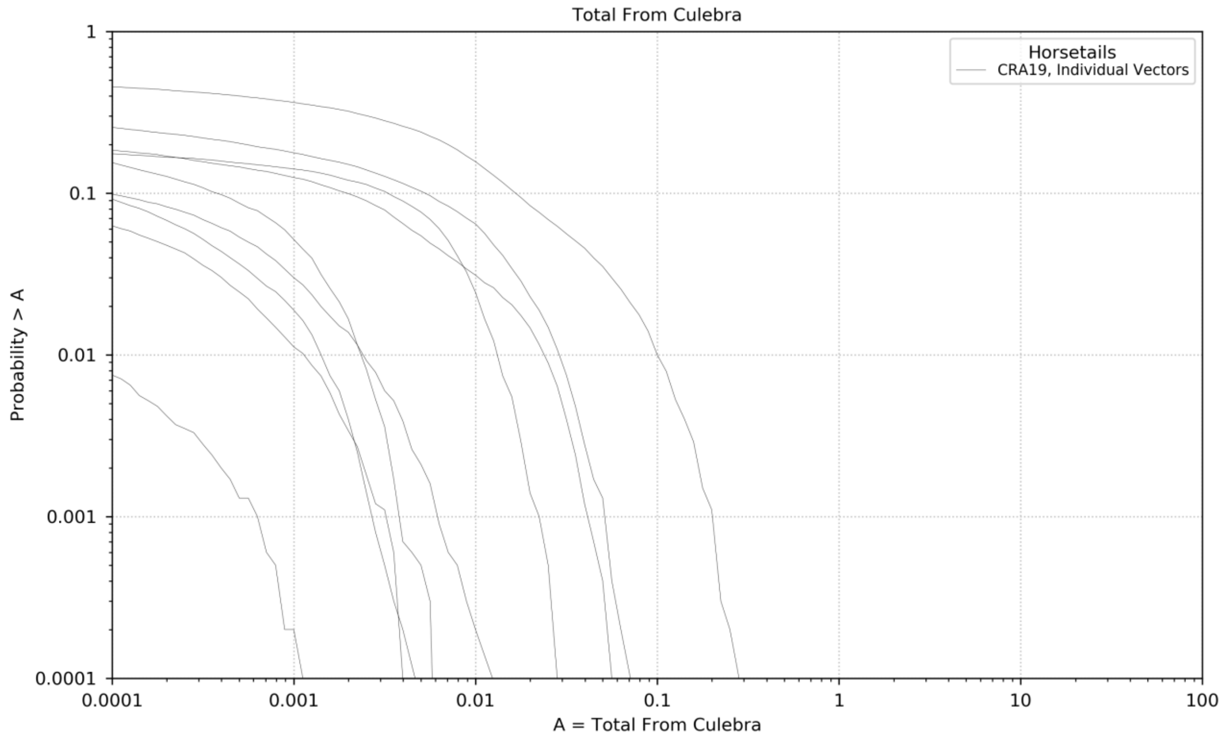

Figure 18 – Replicate 3 Normalized Culebra Transport Releases

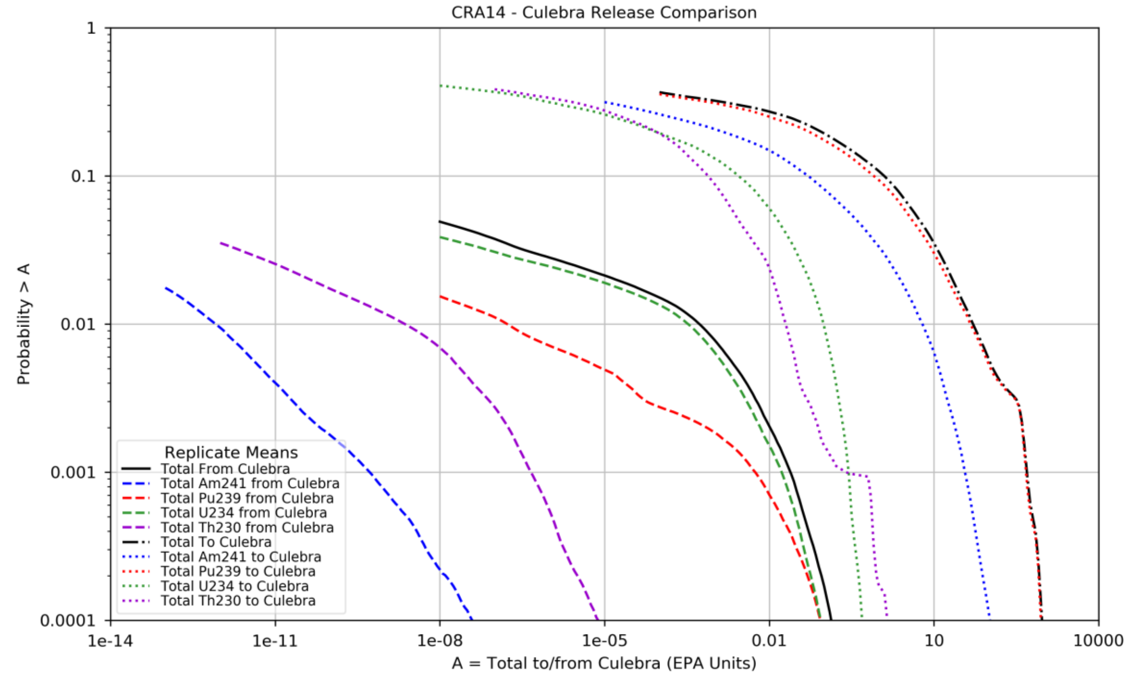

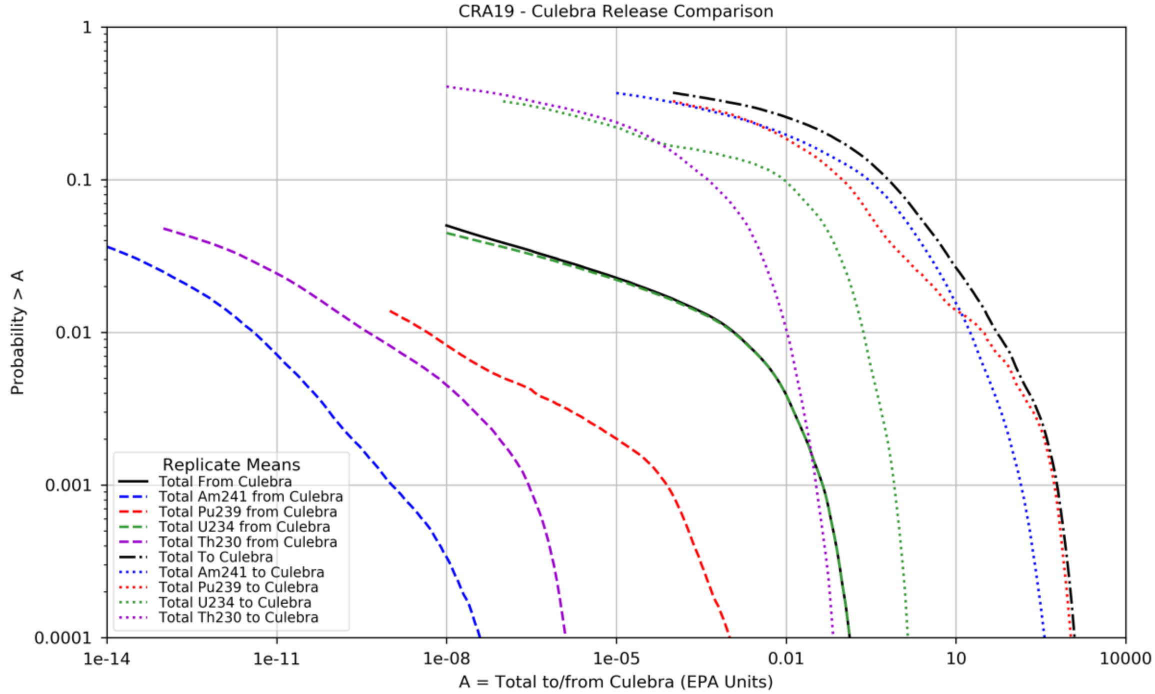

Figure 19 – Mean CCDFs for Releases to and from the Culebra by Radionuclide: CRA14 (top) and CRA19 (bottom)

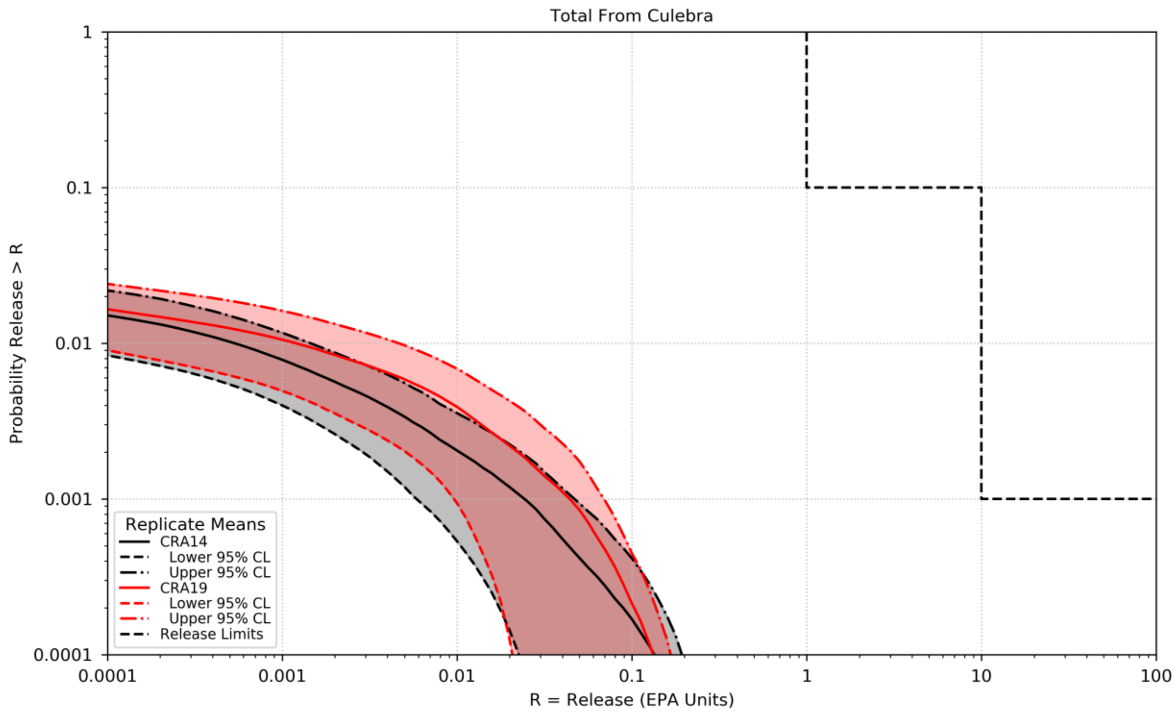

Figure 20 – Confidence Limits on Overall Means for Transport Releases from the Culebra

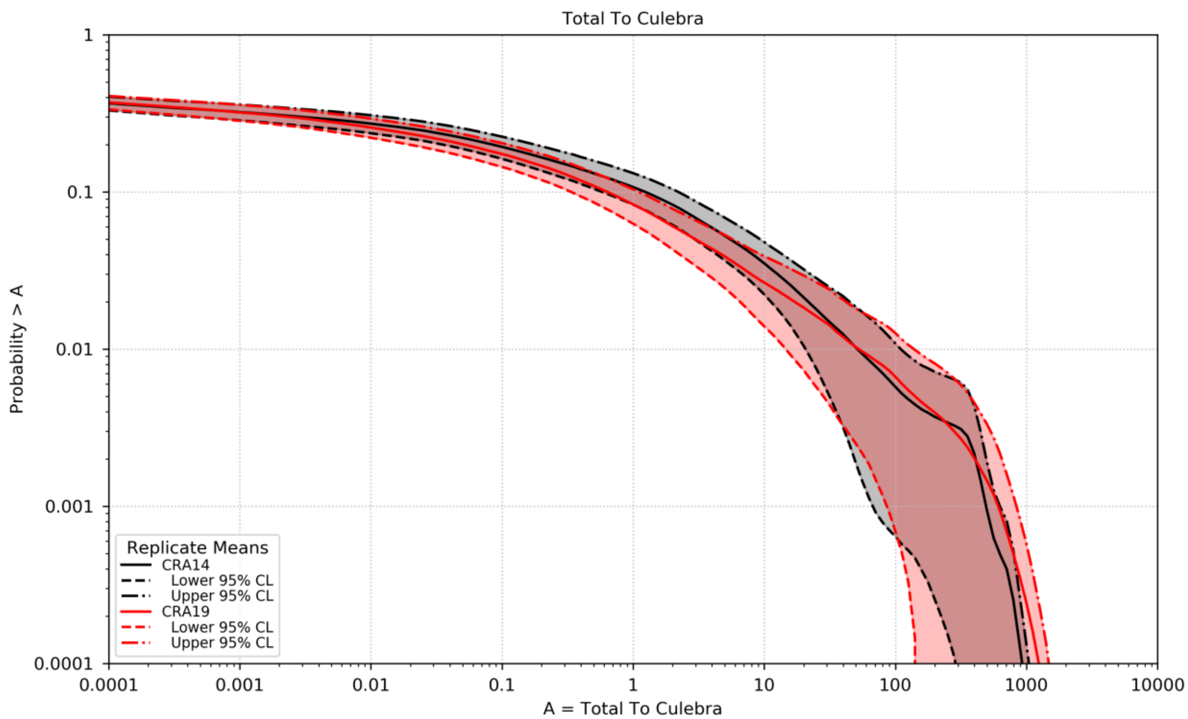

Figure 21 – Confidence Limits on Overall Means for Transport Releases to the Culebra

4.5 Total Normalized Releases

Total normalized releases for a disturbed repository in the CRA-2019 PA are presented in this section and compared to results obtained in the CRA-2014 PA. Total releases are calculated by summing the releases across each potential release pathway, namely cuttings and cavings releases, spallings releases, direct brine releases, and transport releases. As discussed in Sarathi (2019), releases for an undisturbed scenario are negligible and are therefore not included in the calculation of total releases from the repository. The overall mean CCDF is computed as the arithmetic mean of the mean CCDFs from each replicate. Figure 22, Figure 23, and Figure 24 show the CRA-2019 PA CCDFs for total releases in replicates 1, 2, and 3, respectively.

The overall means of the CRA-2019 PA release component contributions are shown in Figure 25. As seen in that figure, total normalized releases obtained for CRA19 are dominated by cuttings and cavings releases at high probabilities (and relatively low consequence) and DBRs at low probabilities (and relatively high consequence). Contributions to total releases from spallings and Culebra transport are not dominant, although spallings and Culebra transport releases have been increased in comparison to CRA14.

Figure 26 shows the 95 percent confidence limits about the overall transport mean for both CRA19 and CRA14, while a comparison of the statistics can be seen in Table 7. Overall, total normalized releases increased from the CRA-2014 PA to the CRA-2019 PA due to increases in all contributing release components. As seen in Figure 26, the overall mean for normalized total releases and its lower/upper 95% confidence limits are well below acceptable release limits. Accordingly, the WIPP remains in compliance with the containment requirements of 40 CFR Part 191.

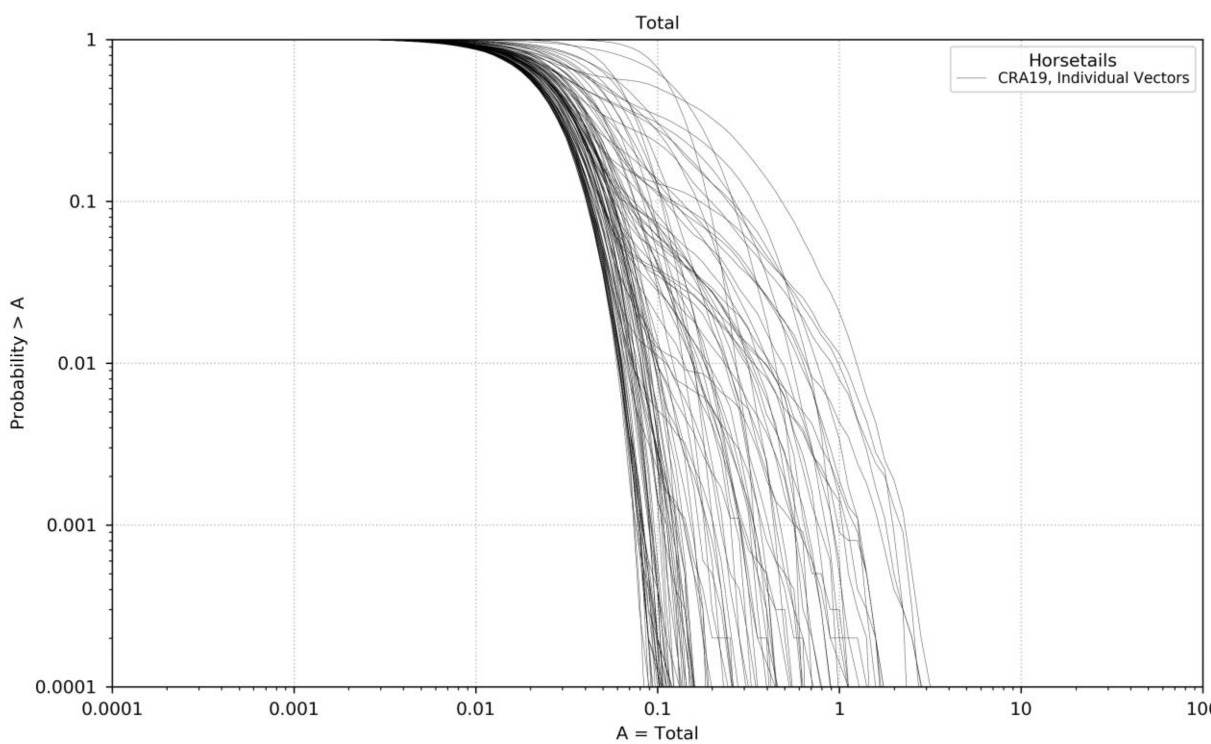

Figure 22 – Replicate 1 Total Normalized Releases

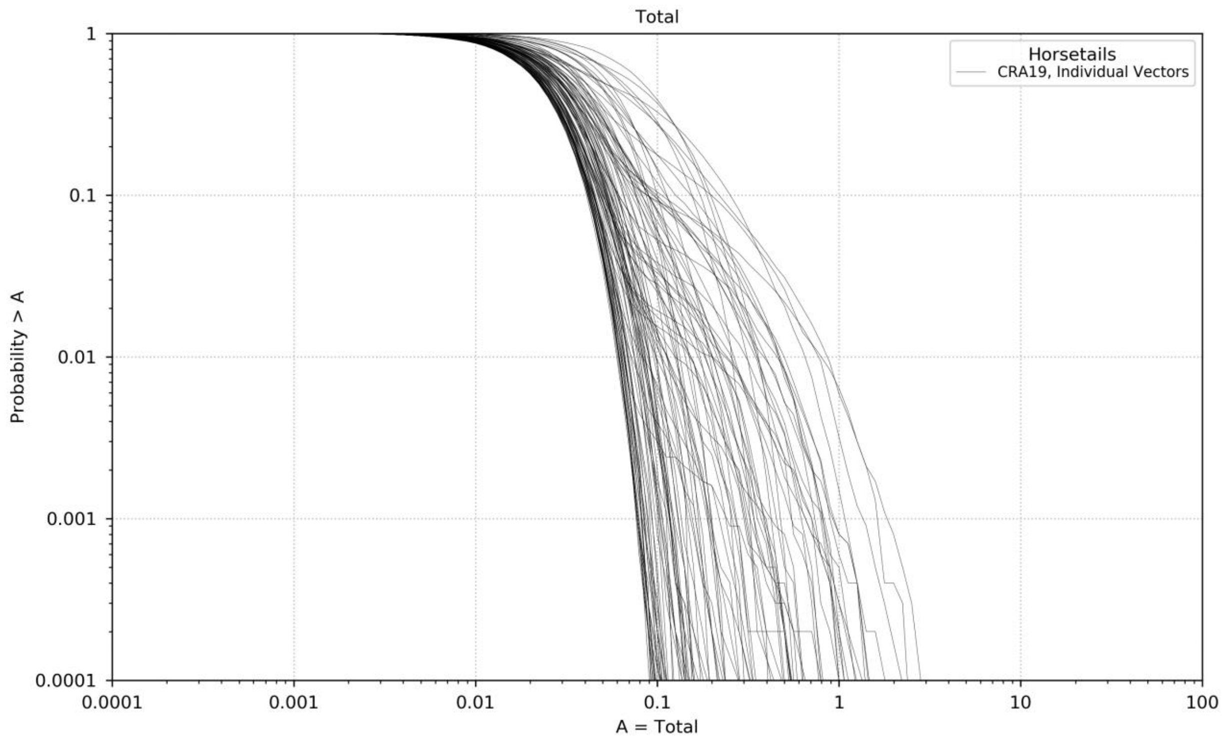

Figure 23 – Replicate 2 Total Normalized Releases

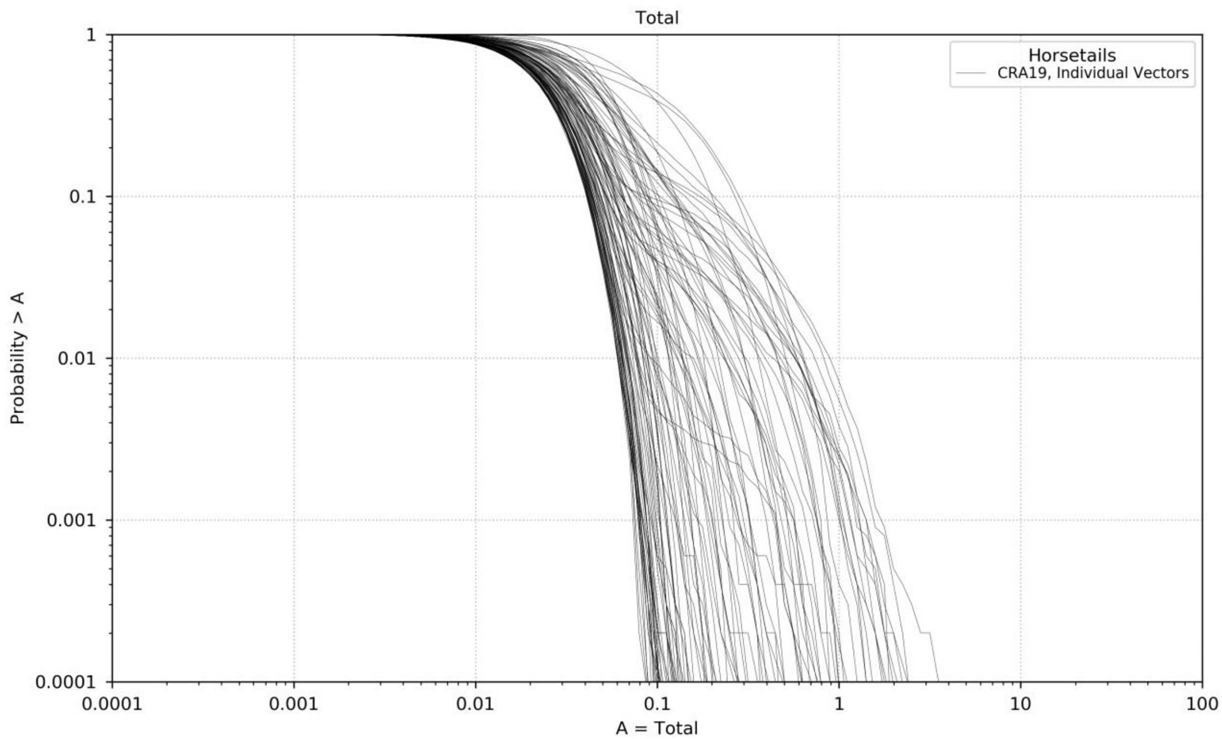

Figure 24 – Replicate 3 Total Normalized Releases

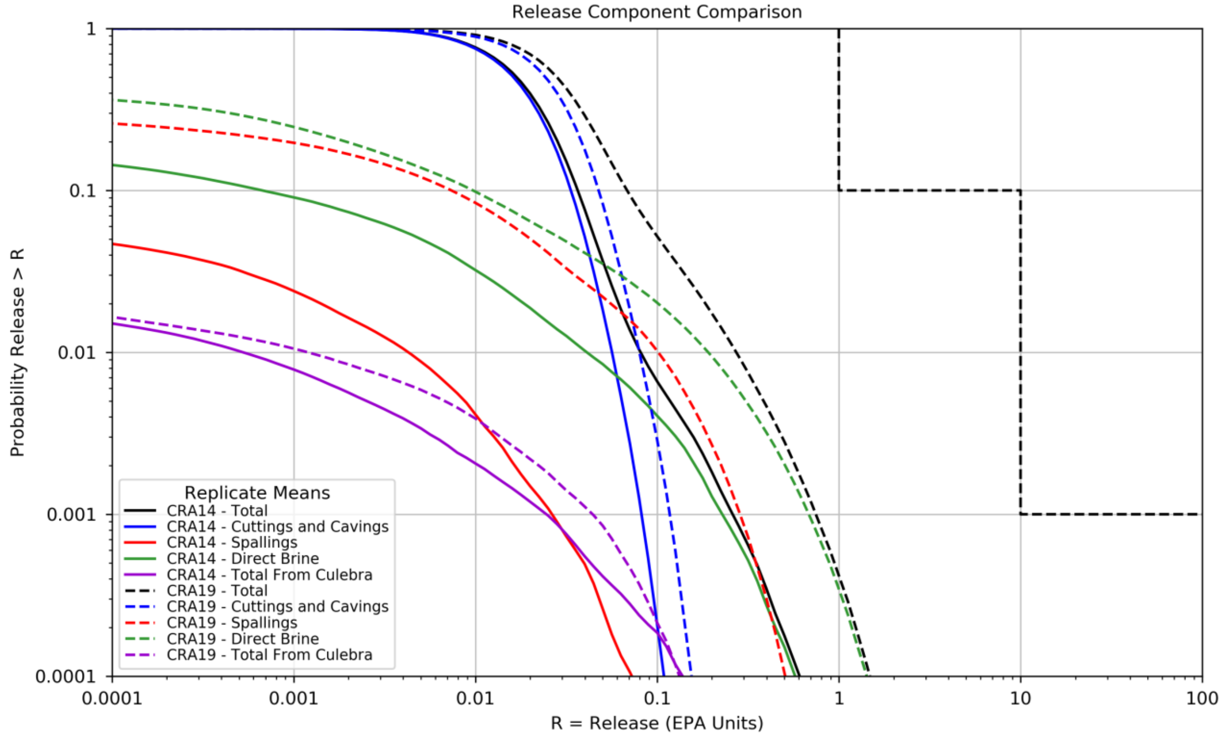

Figure 25 – Comparison of Overall Means for Release Components

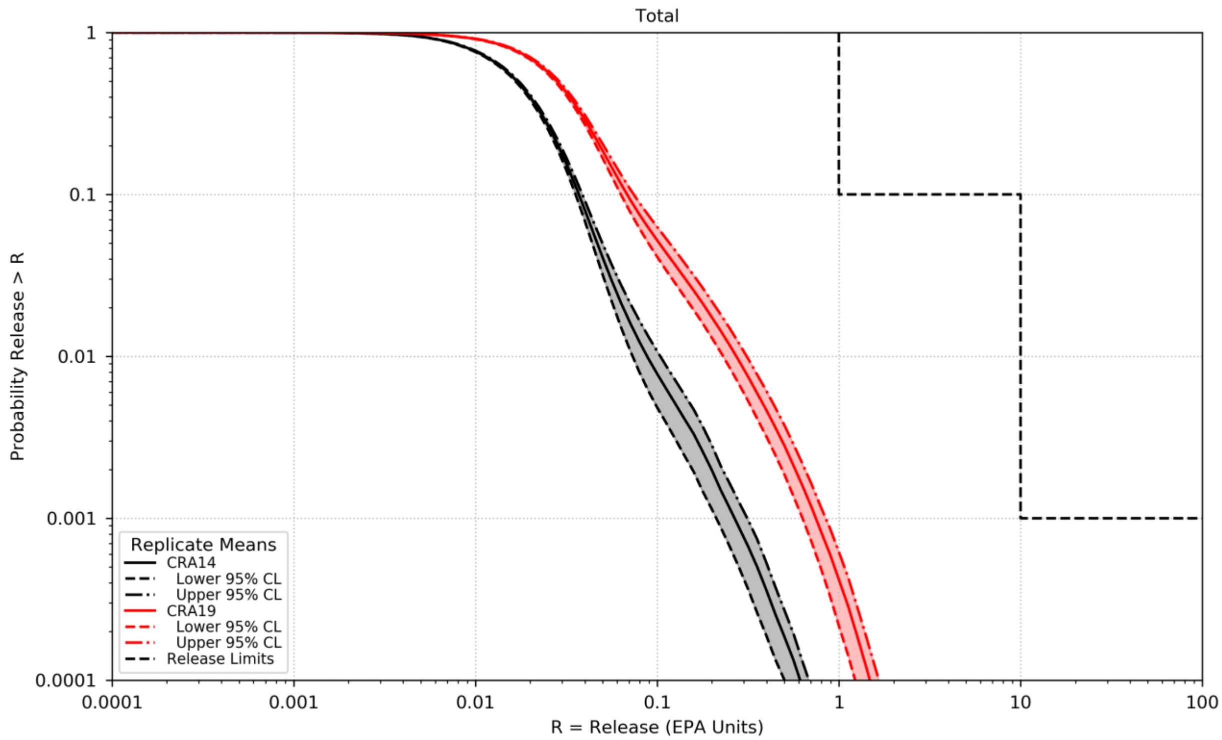

Figure 26 – Confidence Limits on Overall Mean for Total Normalized Releases

Table 7 – Statistics on the Overall Mean for Total Normalized Releases[1]

Probability	Analysis	Mean Total Release	Lower 95% CL	Upper 95% CL	Release Limit
0.1	CRA14	0.0373	0.0355	0.0388	1
	CRA19	0.0685	0.0631	0.0745	
0.001	CRA14	0.2677	0.2124	0.3132	10
	CRA19	0.7505	0.6301	0.8501	

[1] As discussed in Section 1.1.16, the CRA14 values listed here are from CRA14 Rev. 2. The Rev. 2 values represent an approximately 1.6% increase over the CRA14 Rev. 0 value at probability 0.1, and a 2.6% increase at probability 0.001.

5.0 SUMMARY

Changes incorporated into the CRA-2019 PA include planned changes as well as parameter and implementation changes. Of the changes delineated in Section 1.1 as possibly having an impact on the CCDF creation results, the following subset of changes are observed to be associated with the primary differences in releases between CRA-2014 PA and CRA-2019 PA:

- Adapting the APCS approach in the CRA-2019 PA compared to the CRA-2014 PA.
- The addition of brine radiolysis resulted in increased repository pressures, impacting spallings and direct brine releases.
- Refinement to the probability of encountering pressurized brine, which contributed to an increased probability of high-pressure E1 intrusions.
- Update to drilling rate, which increased the number of borehole intrusions modeled.
- Update to plugging pattern parameters, which decreased the probability of E1 and E2 intrusions.

Changes in plugging pattern parameters offset the increases due to the increased drilling rate for all release mechanisms except cuttings and cavings. Cuttings and cavings were mainly impacted by the increased drilling rate. Spallings volumes and releases are increased primarily due to an increase in waste panel pressure. Direct brine releases are higher than those seen in the CRA-2014 PA results due to changes in repository pressure and substantially higher saturations in the "middle" intrusion locations. Total mobile radioactivity concentrations decreased overall, however these decreases were offset by increased DBR volumes. As a result of multiple varying factors, releases to the LWB resulting from subsurface transport of radionuclides through the Culebra are slightly higher in the CRA-2019 PA, although the contribution to the overall mean releases is small. Cuttings and cavings and direct brine releases continue to dominate the total normalized releases.

Overall, total normalized releases calculated in the CRA-2019 PA remain below their regulatory limits. As a result, the WIPP remains in compliance with the containment requirements of 40 CFR Part 191.

This page intentionally left blank.

6.0 REFERENCES

Bethune, J. 2019a. Analysis Package for Direct Brine Releases in the 2019 Compliance Recertification Application Performance Assessment (CRA-2019 PA). Sandia National Laboratories, Carlsbad, NM. ERMS 571370.

Bethune, J. 2019b: Impact of Negative Flux in SECOTP2D, Memorandum to WIPP Records Center, Carlsbad, NM: Sandia National Laboratories. July, 2019. ERMS 571697.

Camphouse, R. 2013. Analysis Plan for the 2014 WIPP Compliance Recertification Application Performance Assessment. Sandia National Laboratories, Carlsbad, NM: ERMS 559198.

Camphouse, R. 2014. Impact Assessment of an Additional WIPP Shaft Sandia National Laboratories, Carlsbad, NM: ERMS 562973.

Clayton, D.J., S. Dunagan, J.W. Garner, A.E. Ismail, T.B. Kirchner, G.R. Kirkes, M.B. Nemer. 2008. Summary Report of the 2009 Compliance Recertification Application Performance Assessment. Sandia National Laboratories, Carlsbad, NM. ERMS 548862.

Clayton, D.J., R.C. Camphouse, J.W. Garner, A.E. Ismail, T.B. Kirchner, K.L. Kuhlman, M.B. Nemer. 2010. Summary Report of the CRA-2009 Performance Assessment Baseline Calculation. Sandia National Laboratories, Carlsbad, NM. ERMS 553039.

Clayton, D.J. 2013. Justification of Chemistry Parameters for Use in BRAGFLO for AP-164, Rev. 1. Sandia National Laboratories, Carlsbad, NM. ERMS 559466.

Cotsworth, E. 2005. EPA Letter on Conducting the Performance Assessment Baseline Change (PABC) Verification Test. U.S. EPA, Office of Radiation and Indoor Air, Washington, D.C. ERMS 538858.

Cotsworth, E. 2009. EPA Letter on CRA-2009 First Set of Completeness Comments. U.S. EPA, Office of Radiation and Indoor Air, Washington, D.C. ERMS 551444.

Day, B. 2018. *Impact Analysis for BRAGFLO 6.03 Software Problem Report, SPR 18-002*. Sandia National Laboratories. Carlsbad, NM. ERMS 570325.

Day, B. 2019a. Reassessment of Need and Parameter Justification for Modeling Gas Generation due to Radiolysis of Brine and Cellulose/Plastic/Rubber in WIPP for CRA-2019. Sandia National Laboratories, Carlsbad, NM. ERMS 570873.

Day, B. 2019b. Analysis Package for Salado Flow in the 2019 Compliance Recertification Application Performance Assessment (CRA-2019 PA). Sandia National Laboratories, Carlsbad, NM. ERMS 571368.

Helton, J. et al. 1998. Uncertainty and Sensitivity Analysis Results Obtained in the 1996 Performance Assessment for the Waste Isolation Pilot Plant. Sandia National Laboratories, Albuquerque, NM. SAND98-0365.

Kicker, D. 2019a. Analysis Package for Cuttings, Cavings, and Spallings in the 2019 Compliance Recertification Application Performance Assessment (CRA-2019 PA). Sandia National Laboratories, Carlsbad, NM. ERMS 571369.

Kicker, D. 2019b. Analysis Package for Inventory EPA Units in the 2019 Compliance Recertification Application Performance Assessment (CRA-2019 PA). Sandia National Laboratories, Carlsbd, NM. ERMS 571372.

Kicker, D. 2019c. Radionuclide Inventory Screening Analysis for the 2019 Compliance Recertification Application Performance Assessment (CRA-2019 PA), Revision 1. Sandia National Laboratories, Carlsbad, NM. ERMS 571659.

Kirchner, T. 2012. AP-162 Revision 0: Analysis Plan for the Migration of the Performance Assessment Codes to the Sun Solaris Blade Server Running with Intel Processors. Sandia National Laboratories, Carlsbad, NM. ERMS 557765.

Kirchner, T., Zeitler, T., and Kirkes, R. 2012. Evaluating the Data in Order to Derive a Value for GLOBAL:PBRINE. Memorandum to Sean Dunagan dated December 11, 2012. Sandia National Laboratories, Carlsbad, NM. ERMS 558724.

Kirchner, T., A. Gilkey, and J. Long. 2014. Summary Report on the Migration of the WIPP PA Codes from VMS to Solaris, AP-162 Revision 1. Sandia National Laboratories, Carlsbad, NM. ERMS 561757.

Kirchner, T., A. Gilkey, and J. Long. 2015. Addendum to the Summary Report on the Migration of the WIPP PA Codes from VMS to Solaris, AP-162. Sandia National Laboratories, Carlsbad, NM. ERMS 564675.

Leigh, C.D., J.F. Kanney, L.H. Brush, J.W. Garner, G.R. Kirkes, T. Lowry, M.B. Nemer, J.S. Stein, E.D. Vugrin, S. Wagner, and T.B. Kirchner. 2005. 2004 Compliance Recertification Application Performance Assessment Baseline Calculation, Revision 0. Sandia National Laboratories, Carlsbad, NM. ERMS 541521.

Long, J. 2013. Execution of Performance Assessment Codes for the CRA-2014 Performance Assessment. Sandia National Laboratories, Carlsbad, NM. ERMS 560016.

Long, J. 2019. Computational Code Execution and File Management for the 2019 Compliance Recertification Application Performance Assessment (CRA-2019 PA). Sandia National Laboratories, Carlsbad, NM. ERMS 571375.

MacKinnon, R.J., and G. Freeze. 1997a. Summary of EPA-Mandated Performance Assessment Verification Test (Replicate 1) and Comparison with the Compliance Certification Application Calculations, Revision 1. Sandia National Laboratories, Carlsbad, NM. ERMS 422595.

MacKinnon, R.J., and G. Freeze. 1997b. Summary of Uncertainty and Sensitivity Analysis Results for the EPA-Mandated Performance Assessment Verification Test, Rev. 1. Sandia National Laboratories, Carlsbad, NM. ERMS 420669.

MacKinnon, R.J., and G. Freeze. 1997c. Supplemental Summary of EPA-Mandated Performance Assessment Verification Test (All Replicates) and Comparison with the Compliance Certification Application Calculations, Revision 1. Sandia National Laboratories, Carlsbad, NM. ERMS 414880.

Peake, Thomas. 1998. Technical Report Review of TDEM Analysis of WIPP Brine Pockets. Prepared for U. S. Environmental Protection Agency, Office of Radiation and Indoor Air, 401 M. Street, S. W., Washington, DC.

Rechard, R. P., A. C. Peterson, J. D. Schreiber, H. J. Iuzzolino, M. S. Tierney and J. S. Sandha. 1991. Preliminary comparison with 40 CFR Part 191, Subpart B for the Waste Isolation Pilot Plant, December 1991; Volume 3: Reference Data. Sandia National Laboratories, Albuquerque, NM.

Sandia National Laboratories (SNL). 2010. Design Document and User's Manual for CCDFGF. Sandia National Laboratories, Carlsbad, NM. ERMS 554046.

Sarathi, R. 2019. Analysis Package for Actinide Mobilization and Salado Transport in the 2019 Compliance Recertification Application Performance Assessment (CRA-2019 PA). Sandia National Laboratories, Carlsbad, NM. ERMS 571371

U.S. Congress. 1992. WIPP Land Withdrawal Act, Public Law 102-579, 106 Stat. 4777, 1992; as amended by Public Law 104-201, 110 Stat. 2422, 1996.

U.S. Department of Energy (DOE) 1996. Title 40 CFR Part 191 Compliance Certification Application for the Waste Isolation Pilot. U.S. Department of Energy Waste Isolation Pilot Plant, Carlsbad Area Office, Carlsbad, NM. DOE/CAO-1996-2184.

U.S. Department of Energy (DOE) 2004. Title 40 CFR Part 191 Compliance Recertification Application for the Waste Isolation Pilot Plant, 10 vols., U.S. Department of Energy Waste Isolation Pilot Plant, Carlsbad Area Office, Carlsbad, NM. DOE/WIPP 2004-3231.

U.S. Department of Energy (DOE). 2016. WIPP UPDATE: October 14, 2016, Plans Call for Controlled Withdrawal from South End of Underground. https://www.wipp.energy.gov/Special/WIPP%20Update%2010_14_16.pdf

U.S. Department of Energy (DOE). 2017. Sandia Recommendation for Completion of Fully-Qualified RPC2 Calculations. Email from R. Patterson to P. Shoemaker dated February 7, 2017.

U.S. Department of Energy (DOE). 2018. Delaware Basin Monitoring Annual Report. DOE/WIPP-18-2308, Rev. 1.

U.S. Environmental Protection Agency (EPA). 1996. 40 CFR Part 194: Criteria for the Certification and Recertification of the Waste Isolation Pilot Plant's Compliance with the 40 CFR Part 191 Disposal Regulations; Final Rule. Federal Register, Vol. 61, 5223-5245.

U.S. Environmental Protection Agency (EPA). 1998. 40 CFR 194, Criteria for the Certification and Recertification of the Waste Isolation Pilot Plant's Compliance with the Disposal Regulations: Certification Decision: Final Rule, Federal Register. Vol. 63, 27354-27406.

U.S. Environmental Protection Agency (EPA). 2006. 40 CFR 194, Criteria for the Certification and Recertification of the Waste Isolation Pilot Plant's Compliance with the Disposal Regulations: Certification Decision: Final Rule, Federal Register. Vol. 71, 18010-18021.

U.S. Environmental Protection Agency (EPA). 2010. 40 CFR Part 194 Criteria for the Certification and Recertification of the Waste Isolation Pilot Plant's Compliance With the Disposal Regulations: Recertification Decision, Federal Register No. 222, Vol. 75, pp. 70584-70595, November 18, 2010.

U.S. Environmental Protection Agency (EPA). 2017a. Criteria for the Certification and Recertification of the Waste Isolation Pilot Plant's Compliance with the Disposal Regulations; Recertification Decision. July 19, 2017. Office of Radiation and Indoor Air, Docket EPA-HQ-OAR-2014-0609-0079.

U.S. Environmental Protection Agency (EPA). 2017b. Probability of Encountering Castile Brine Beneath the WIPP Waste Panels Using the TDEM Block Method. June, 2017. Office of Radiation and Indoor Air, Docket EPA-HQ-OAR-2014-0609-0047.

U.S. Environmental Protection Agency (EPA). 2017c. Technical Support Document for Section 194.24, Evaluation of the Compliance Recertification Actinide Source Term, Gas Generation, Backfill Efficacy, Water Balance and Culebra Dolomite Distribution Coefficient Values. June 2017. Office of Radiation and Indoor Air, Docket EPA-HQ-OAR-2014-0609-0054.

Van Soest, G.D. 2018. Performance Assessment Inventory Report – 2018. Los Alamos National Laboratory Carlsbad Operations. Carlsbad, NM. LA-UR-18-31882.

WIPP PA. 2010. Requirements Document for CCDFGF (Version 7.0). Sandia National Laboratories. Carlsbad, NM: ERMS 554044.

Zeitler, T.R and B. Day. 2016. CRA14_SEN4 Sensitivity Study, Rev. 1. Sandia National Laboratories. Carlsbad, NM. ERMS 567505.

Zeitler, T.R and B. Day. 2017. Analysis Plan for the Assessment of Abandoned Panel Closures in South End of Repository and Lack of Waste Emplacement in Panel 9. Sandia National Laboratories. Carlsbad, NM. ERMS 568138.

Zeitler, T.R, B. Day, J. Bethune, R. Sarathi, J. Long. 2017. Assessment of Abandoned Panel Closures in South End of Repository and Lack of Waste Emplacement in Panel 9. Sandia National Laboratories. Carlsbad, NM. ERMS 568459.

Zeitler, T.R. 2019a. Calculation of Shaft and Experimental Area Dimensions for Use in the CRA-2019 PA. Sandia National Laboratories. Carlsbad, NM. ERMS 571045.

Zeitler, T.R. 2019b. A Summary of EPA/DOE Defined Parameters to be Implemented in the CRA-2019 PA. Sandia National Laboratories. Carlsbad, NM. ERMS 570879.

Zeitler, T.R. 2019c. Analysis Plan for the 2019 WIPP Compliance Recertification Application Performance Assessment. Sandia National Laboratories, Carlsbad, NM. ERMS 571150.